
I 8

Oceanic Analogues of Large-scale Atmospheric Motions

*Jule G. Charney and
Glenn R. Flierl*

18.1 Introduction

Newton (1687, book 2, propositions 48–50) and Laplace (1799) were aware that the principles governing the ocean tides would also govern the atmospheric tides. Helmholtz (1889) showed that ocean waves and billow clouds were manifestations of the same hydrodynamic instability, and he speculated that storms were caused by a similar instability. Had he known the structure of the Gulf Streams meanders, he might have speculated on their dynamic similarities to storms as well. Such intercomparisons were natural to the great hydrodynamicists of the past who took the entire universe of fluid phenomena as their domain. Although a degree of provincialism was introduced in the late nineteenth and early twentieth centuries by the exigencies of weather forecasting, it was just the practical requirements of weather observation that stimulated the development of modern dynamic meteorology and led to the deepening of its connections with physical oceanography. The recent explosive growth of the three-dimensional data base, the exploration of other planetary atmospheres, and the resulting increase in theoretical activity have greatly extended the list of ocean-atmosphere analogues. Indeed, it is now no exaggeration to say that there is scarcely a fluid dynamical phenomenon in planetary atmospheres that does not have its counterpart in the oceans and vice versa. This had led to the discipline, geophysical fluid dynamics, whose guiding principles are intended to apply equally to oceans and atmospheres.

Within this discipline the dominance of the earth's rotation defines a subclass of large-scale phenomena whose dynamics may for the most part be derived from quasi-geostrophy. For several years the authors have conducted a graduate course at MIT on the dynamics of large-scale ocean and atmospheric circulations in the belief that a parallel consideration of large-scale oceanic and atmospheric motions would broaden the range of our students' experience and deepen their understanding of the principles of fluid geophysics. C.-G. Rossby (1951) put the matter well:

It is fairly certain that the final formulation of a comprehensive theory for the general circulation of the atmosphere will require intimate cooperation between meteorologists and oceanographers. The fundamental problems associated with the heat, mass and momentum transfer at the sea surface concern both these sciences and demand a joint effort for their solution. However, an even stronger reason for that pooling of intellectual resources . . . may be found in the fact that the various theoretical analyses of the large-scale oceanic and atmospheric circulation patterns which have been called into being by our sudden wealth of observational data, appear to have so much in common that they may be looked upon as different facets of one broad general study, the ultimate aim of which might

be described as an attempt to formulate a comprehensive theory for fluid motion in planetary envelopes.

He went on to say that "comparisons between the circulation patterns in the atmosphere and in the oceans provide us with a highly useful substitute for experiments with controlled variations of the fundamental parameters."

Needless to say, we subscribe to Rossby's views and therefore have willingly undertaken the task of reviewing the fluid dynamics of a number of phenomena that have found explanation in one medium and are deemed to have important analogues in the other. Where the analogues have already been explained, we have given a brief review of some of their salient features, but where little is known, we have not refrained from interpolating simple models or speculations of our own. In doing so, we were aware that the subject has grown so large that it includes most of geophysical fluid dynamics, and that, even if it were limited to large-scale, quasi-geostrophic motions, it could not be encompassed in a review article of modest size. At least two excellent review articles on this topic, by N. Phillips (1963) and by H.-L. Kuo (1973), have already appeared, and there is now a text by Pedlosky (1979a) on geophysical fluid dynamics. For these reasons we have decided to limit ourselves to a small number of topics having to do primarily with disturbances of the principal atmospheric and oceanic currents, their propagation characteristics, their interactions with the embedding currents, and, to a lesser degree, with their self-interactions.

It is perhaps no accident that both Phillips and Kuo are meteorologists. Dynamic meteorology has benefited from a wealth of observational detail that has been denied to physical oceanography. Consequently, meteorologists have been the first to observe and explain many typical large-scale phenomena. This has by no means always been the case, but it has been so sufficiently often to justify the title of our review.

18.2 The General Circulations of Oceans and Atmospheres Compared

If it had been possible in a meaningful way, it would have been useful and instructive to make detailed dynamical comparisons of the general circulations of the atmosphere and oceans. This has not been so, and we must content ourselves with a few general remarks. Because of its relative transparency to solar radiation, the earth's atmosphere is heated from below; the oceans, like the relatively opaque atmosphere of Venus, are heated from above. The differential heating of the atmosphere produces a mean circulation that carries heat upward and poleward. Its baroclinic instabilities do likewise. These heat transports, combined with in-

ternal radiative heat transfer, tend to stabilize the atmosphere statically, and their effects are augmented by moist convection which drives the temperature lapse-rate toward the moist-adiabatic. The net result is that the atmosphere is rather uniformly stable for dry processes up to the tropopause. Above the tropopause, it is made increasingly more stable by absorption of solar ultraviolet radiation in the ozone layer. The oceans are rendered statically stable by heating from above, but heating cannot take place everywhere because the oceans, unlike the atmosphere, cannot dispose of internal heat by radiation to space; they must carry it back to the surface layers, where it can be lost by surface cooling. The most stable parts of the oceans are in the subtropical gyres, where the oceans are heated and Ekman pumping transfers the heat downward. The least stable parts are in the polar regions, where cold water is formed and carried downward by convection. The atmospheric troposphere has sometimes been compared with the waters above the thermocline, the tropopause with the thermocline, and the stratosphere with the deep waters below the thermocline (cf. Defant, 1961b). This comparison may be justified by the fact that it is in the atmospheric and oceanic tropospheres that the horizontal temperature gradients and the kinetic and potential energy densities are greatest. But from the standpoint of static stability, the absorption of radiation at the surface of the oceans makes its upper layers more analogous to the stratosphere. The static stability for the bulk of the atmosphere and oceans is determined by deep convection occurring in small regions. The analogy between deep convection in the atmosphere and deep convection in the oceans is between the narrow intertropical convergence zones over the oceans and the limited areas of cumulus convection over the tropical continents on the one hand, and the limited regions of deep-water formation in the polar seas on the other. From this standpoint, the ocean waters below the thermocline are more analogous to the atmospheric troposphere. Both volumes comprise more than 80% of the total by mass and both are controlled by deep convection.

It is remarkable that the regions of pronounced rising motion in the atmosphere and sinking motion in the oceans are so confined horizontally. Stommel (1962b) was the first to offer an explanation for the smallness of the regions of deep-water formation. His work motivated several attempts to explain the asymmetries in the circulation of a fluid heated differentially from above or below. We may cite as examples the experimental work of H. T. Rossby (1965) and the theoretical work of Killworth and Manins (1980) on laboratory fluid systems, and the papers of Goody and Robinson (1966) and Stone (1968) on the upper circulation of Venus. Because of its cloudiness, Venus has been assumed to be heated primarily from above, although it

now is known that sunlight does penetrate into the lower Venus atmosphere and that the high temperatures near the surface are due to a pronounced greenhouse effect (Keldysh, 1977; Young and Pollack, 1977; Tomasko, Doose, and Smith, 1979). When a fluid is heated from below, the rising branches are found to be narrow and the sinking branches broad; when it is heated from above the reverse is true. One may offer the qualitative explanation that it is the branch of the circulation that leaves the boundary and carries with it the properties of the boundary that has the greatest influence on the temperature of the fluid as a whole: convection is more powerful than diffusion. In the case of differential heating from below, the rising warm branch causes most of the fluid to be warm relative to the boundary and therefore gravitationally stable except in a narrow zone at the extreme of heating where the intense rising motion must occur. In the case of differential heating from above, the sinking cold branch causes the bulk of the fluid to be cold and gravitationally stable except in a narrow region at the extreme of cooling where the intense sinking motion must occur. Theoretical models of axisymmetric, thermally driven (Hadley) circulations in the atmosphere (Charney, 1973) show the same effect: a narrow rising branch and a broad sinking branch. This effect is strengthened by cumulus convection (Charney, 1969, 1971b; Bates, 1970; Schneider, 1977). The narrow rising branch of the Hadley circulation directly controls the dynamic and thermodynamic properties of the tropics and subtropics and indirectly influences the higher-latitude circulations. Similarly, the small sinking branches of the ocean circulation determine the near-homogeneous deep-water properties as well as some of the intermediate-water properties. But there is a difference: we know how the heat released in the ascending branch of the Hadley circulation is disposed of; we do not know how the cold water in the abyssal circulation is heated. Whatever the process, the existence of a preponderant mass of near-homogeneous water at depth forces great static stability in the shallow upper regions of the ocean. It demands a thermocline.

Again we have an analogy between the upper circulation of the oceans and the upper circulation of Venus. Rivas (1973, 1975) has shown that the intense circulation of Venus is confined to a thin layer within and just below the region of intense heating and cooling by radiation. The more or less independent circulation produced by the separate heat sources of the atmospheric stratosphere is similarly analogous to the upper ocean circulation. And here there is an atmosphere-ocean analogy pertaining to our knowledge of transfer processes. While the mechanisms of heat transfer in the stratosphere are fairly well known, the mechanism of transfer of thermally inactive gases or suspended

particles is not, for the latter involves a knowledge of particle trajectories, which are not easily determined. The large-scale eddies in the atmosphere, insofar as they are nondissipative, cannot transfer a conserved quantity across isentropic surfaces. Thermal dissipation is required for parcels to move from the low-entropy troposphere to the high-entropy stratosphere. Atmospheric chemists sometimes postulate an ad hoc turbulent diffusion to explain the necessary vertical transfers of such substances as the oxides of nitrogen and the chlorofluoromethanes into the ozone layers. But it is doubtful whether this type of diffusion is needed to account for the actual transfer, because there already exists the nonconservative mechanism of radiative heat transfer, and this, together with the large-scale eddying motion, can by itself account for the transfers (Andrews and McIntyre, 1978a; Matsuno and Nakamura, 1979). The analogous oceanic problem has already been mentioned: how is heat or salt transferred from the deep ocean layers into the upper wind-stirred layers? The cold deep water produced in the polar seas and the intermediate salty water produced in the Mediterranean Sea must eventually find their way by dissipative processes to the surface, where they can be heated or diluted. While a number of internal dissipation mechanisms have been proposed in a speculative way (double diffusion, low-Richardson-number instability zones, internal-wave breaking) one may invoke Occam's razor, as has been done so successfully to explain the Gulf Stream as an inertial rather than a frictional boundary layer (Charney, 1955b; Morgan, 1956) and postulate no internal dissipative mechanism at all. Then, outside of the convective zones, properties will be advected by the mean flow or by eddies along isentropic surfaces, and move from one such surface to another only at the boundaries of the ocean basins where we may assume turbulent dissipation does occur. It would be interesting to see how far one could go with boundary dissipation alone. Welander (1959) and Robinson and Welander (1963) have taken a first step by investigating the motions of a conservative system communicating only with an upper mixed layer.

18.3 The Transient Motions

Meteorologists, pressed with the necessity of forecasting the daily weather, have always been concerned with the transient motions of the atmosphere. Attempts to understand the processes leading to growth, equilibration, translation and decay of these "synoptic-scale" (order 1000 km) eddies¹ have produced theories of baroclinic instability (Charney, 1947; Eady, 1949), Rossby wave motion (Rossby et al., 1939; Haurwitz, 1940b) and Ekman pumping (Charney and Eliassen, 1949). It was first recognized by Jeffreys (1926) and

demonstrated conclusively by Starr (1954, 1957) and Bjerknæs (1955, 1957) that the dynamics of the mean circulation are strongly influenced by the transports of heat and zonal momentum by the eddies [for a review of these developments, see Lorenz (1967)]. This has prompted research on eddy dynamics and also on the parameterization of eddy fluxes (cf. Green, 1970; Rhines, 1977; Stone, 1978; Welander, 1973).

The study of eddy motions in the ocean is a new development. Although the existence of fluctuations in the Gulf Stream was reported by early observers such as Laval (1728) and Rennell (1832), actual *prediction* of ocean eddies has never been a particularly profitable exercise (perhaps the recent interest of yachtsmen in Gulf Stream rings may presage a change). The serious study of deep ocean fluctuations really began with M. Swallow (1961), Crease (1962), and J. Swallow (1971). At this point, oceanographers began to realize that the mid-ocean variable velocities were not, as might perhaps have been reasonably inferred from atmospheric experience, comparable to the mean flows but rather were an order of magnitude larger. This has spurred intensive experimental and theoretical investigations of the dynamics of the oceanic eddies and their roles in the general circulation (see chapter 11).

Comparisons between the oceanic and atmospheric eddies may be made in respect to their generation, propagation, interaction (both eddy-mean flow and eddy-eddy) and decay. In the sections below we shall describe some of the theoretical approaches to these problems.

In the atmosphere, energy conversion estimates (cf. Oort and Peixoto, 1974) clearly show a transformation of zonal-available potential energy into eddy-available potential energy, then into eddy kinetic energy and finally into heat by dissipation, with some transfer from eddy to zonal kinetic energy. The similarity of the growth phase of this cycle to that exhibited in the theory of small traveling perturbations of a baroclinically unstable (but barotropically stable) flow, leads naturally to the identification of the source of the waves as the baroclinic instability of the zonal flow. This idea has been supported further by the fact that the energy spectrum has peaks near zonal wavenumber six, which simple models predict to be the most rapidly growing wavenumber. However, attempts to apply these models directly to the atmosphere lead to problems: one expects that nonuniform mean flows, non-homogeneous surface conditions, variable horizontal and vertical shears, etc., will alter the dynamics; and one may also wonder about the applicability of the small perturbation-normal mode approach.

The topographically and thermally forced standing eddies also draw upon zonal available potential energy (Holopainen, 1970). The processes by which they do this are not yet clearly understood; they may be related

to the form-drag instability to be described in section 18.7.3. The standing eddies, like the transient eddies, also transport heat and momentum.

Overall energetic analyses have not been applied to oceanic data. However, budgets for basin-averaged kinetic and potential energy have been calculated for the "eddy-resolving general circulation models." These are reviewed by Harrison (1979b). In all but one of the 21 cases he considered, the eddy kinetic energy came from *both* mean kinetic and mean potential energy. Collectively, the eddies seem to be acting as dissipative mechanisms, but Harrison cautions that because the model statistics are inhomogeneous, the overall results may not be representative of the actual dynamics in any limited region. Indeed, the eddies may be acting as a negative viscosity in parts of the domain. Thus, Holland (1978) suggests that the eddies generated in the upper layer of his two-layer model drive the mean flows in the lower layer.

Oceanographers have examined local energy balances. The best known of these studies, by Webster (1961a), has often been interpreted as an indication that the Gulf Stream is accelerated by the eddies. However, Schmitz and Niiler (1969) have pointed out that the cross stream-averaged value of $\overline{u'v'v_x}$ is not distinguishable from zero, so that Webster's results may be an indication merely of transfer of energy from the offshore to the onshore side of the jet and not a mean-flow generation. Even this result is not unambiguous, since the divergence term $(\overline{u'v'v_x})_x$ is not small compared to the terms $-(\overline{u'v'})_x \bar{v}$ and $\overline{u'v'v_x}$, representing, respectively, the eddy-mean flow and the mean flow-eddy conversions. The same problem occurs in attempts to compute regional energy budgets in numerical models (cf. Harrison and Robinson, 1978) unless considerable care is taken.

The conversion of mean-flow potential energy is sometimes inferred from the tilting of the phase lines of the temperature wave with height. This tilt is taken as evidence that the wave is growing by baroclinic instability of the mean flow. Here one must be careful: it is the lagging of the temperature wave behind the pressure wave and the consequent tilting of the phase line of the pressure trough toward the cold air that is important; the temperature phase line may tilt in any direction or not at all. Thus in the Eady model of baroclinic instability the temperature wave has the opposite slope from the pressure wave, whereas in the Charney model it has the opposite slope at low levels and the same slope at high levels (Charney, 1973, chapter IX). It is appropriate, then, to caution that the oceanically most readily available quantity, the phase change of the buoyancy (or entropy) with height, may not lead to a straightforward determination of the sign of the buoyancy flux.

This discussion should make it clear that very little is settled concerning the source of the eddies in the ocean and their effects on the mean flow. "Local" generation mechanisms, such as baroclinic or barotropic instability, flow over topography, and wind forcing are still being considered, and atmospheric analogues are much in mind. But the fact that the transient atmospheric perturbation velocities are comparable to those of the mean flow, whereas the particle speeds for mid-ocean mesoscale eddies are an order of magnitude greater than the mean speeds, suggests that energy may be generated only in limited regions (e.g., the western boundary currents) and propagate from there to other regions.

Oceanic eddies propagate in much the same manner as atmospheric eddies, although there are differences because of the upper-surface boundary conditions: atmospheric waves may propagate upward without reflection, whereas oceanic waves are reflected at the upper boundary. In the atmosphere, the potential vorticity gradients associated with the mean flow play an important role in determining the vertical structure and horizontal propagation for atmospheric waves, whereas this role is played primarily by the gradient of the earth's vorticity for mid-oceanic waves.

The interaction mechanisms may be classified as wave-mean flow interactions and wave-wave interactions. As mentioned above, the concrete evidence for significant wave-mean flow interaction is much greater for the atmosphere than for the ocean. There is not, of course, much oceanic data—Reynolds stresses have been calculated only along a few north-south sections (Schmitz, 1977). Moreover, these records are not very long and the spatial resolution is not sufficient to compute accurate gradients of the Reynolds stresses (given the great inhomogeneity).

The wave-wave interactions, however, seem similar in the two media. The crucial parameter is the Rossby wave steepness parameter $M = U/\beta L^2$, which distinguishes wavelike regimes ($M < 1$) from more turbulent ($M > 1$) regimes as illustrated in the experiments of Rhines (1975).² The oceans are similar to the atmosphere in that this parameter is of order unity for both, although it appears to vary considerably from one oceanic region to another.

The physical mechanisms for dissipation of atmospheric and oceanic eddies are thought to be similar with respect to bottom friction and transfer of energy to gravity wave motions or turbulence (though radiation is a further factor in damping atmosphere waves), but their relative importance may be quite different. The crucial differences for the large-scale circulations between the atmosphere and the ocean may not be in the details of the dissipation mechanisms but rather in their overall time scales. In the atmosphere, damping times are of the order of a few days, comparable to the

eddy velocity advection time L/U , whereas the damping time in the ocean may be as long as several years (cf. Cheney and Richardson, 1976) while the advection time is of the order of a week.

18.4 The Geostrophic Formalism

18.4.1 The Development of the Geostrophic Formalism

The discovery that the atmospheric winds are approximately geostrophic is usually attributed to Buys Ballot (1857). Ferrel (1856) suggested that ocean currents might also have this property. But it took nearly a century before this knowledge was used dynamically. Because the geostrophic and hydrostatic equations express only a condition of balance, it is necessary to consider the slight imbalances produced by forcing, dissipation, and transience in order to predict the evolution and to understand the processes that maintain the balance. One of the first to exploit geostrophy was Bjerknes (1937) in a seminal work on the upper tropospheric long waves and their role in cyclogenesis. Basing his analysis on semiempirical considerations of the gradient wind and the variation with latitude of the Coriolis parameter, he gave the first explanation of the eastward propagation of the upper wave at a speed slower than the mean wind. It was this work that led Rossby et al. (1939) to their vorticity analysis of the upper wave as an independent entity in planar flow. Charney (1947) and Eady (1949) derived quasigeostrophic equations in their analyses of baroclinic instability for long atmospheric waves. General derivations of these equations for arbitrary motions were presented by Charney (1948), Eliassen (1949), Obukhov (1949), and Burger (1958). A particularly simple form which will be used in this review was given by Charney (1962) and Charney and Stern (1962).

In addition to these commonly used approximations, there have been a number of simplifications of the equations of motion which apply the concept of near-geostrophic balance in a less restrictive form. When flows become nongeostrophic in one horizontal dimension while remaining geostrophic in the other, as in frontogenesis, flow over two-dimensional mountain barriers, and in the western boundary currents of the oceans, a set of "semigeostrophic" equations derived from Eliassen's original formulation has often been found useful (Robinson and Niiler, 1967; Hoskins, 1975). Both the quasi- and semigeostrophic equations are special cases of the "balance equations" proposed by Bolin (1955), Charney (1955c, 1962), P. Thompson (1956), and Lorenz (1960). They may be derived from the consideration that in a large class of atmospheric flows the constraints of the earth's rotation and/or gravitational stability so inhibit vertical motion that the horizontal flow, even when it is not quasi-geo-

strophic, remains quasi-nondivergent. The equations derived by Eliassen (1952) for slow thermally and frictionally driven circulations in a circular vortex are a special case of the balance equations; they represent the laws of conservation of angular momentum and entropy and the requirement of equilibrium among the meridional components of the pressure, gravity, and centrifugal forces. For the equilibrium condition to be valid, the flow must be gravitationally and inertially stable. This implies that the potential vorticity must be positive in the northern hemisphere and negative in the southern hemisphere, and it may be shown that this condition on the potential vorticity is also required for the general asymmetric case.

One must also explain why external sources of energy excite quasi-geostrophic flows rather than gravity wave motions to begin with and why so little energy is transferred by nonlinear interactions into the gravity modes afterward. The tendency toward geostrophy is sometimes explained as an adjustment of an initially unbalanced flow by radiation of gravity waves in the manner discussed by Rossby (1938) (see also Blumen, 1968). However, since much of the forcing is applied slowly, rather than impulsively, the calculations of Veronis and Stommel (1956), who consider the nature of the exciting forces, are perhaps more relevant. They showed that the flows will be geostrophically balanced when the forcing period is very large compared to the inertial period. Thus we expect most of the energy will go into geostrophic motions.

The question of how much transfer occurs from geostrophic to nongeostrophic motions through nonlinear interactions remains a matter of concern. Errico's (1979) work suggests that equipartition of energy between gravity waves and geostrophic motions will occur in a conservative, rotating system in statistical equilibrium at sufficiently high energy. But in dissipative systems resembling the atmosphere and oceans, the energy will remain in the geostrophic modes because the gravity waves are dissipated on time scales that are small in comparison with those of their generation. This problem has elements in common with the so-called initialization problem in numerical weather prediction: to find initial values of a flow field that are at once compatible with the incomplete data and at the same time minimize the initial gravity-wave energy and its production rate (cf. Machenhauer, 1977; Daley, 1978).

The problems of transfer from geostrophic into gravity-wave energy are related to those of the production of hydrodynamic noise by a turbulent flow, first studied by Lighthill (1952). An excellent review is presented by Ffowcs Williams (1969). Here the problem is to calculate the generation of acoustic energy in a turbulent flow in which most of the energy resides in nondivergent motions. Since the turbulence is confined

within a limited domain and radiates sound waves into the surrounding medium, there is no possibility of equipartition. An atmospheric or oceanographic analogy to the Lighthill problem would be the generation of internal gravity waves by turbulence in a planetary boundary layer (Townsend, 1965), except that here the generation takes place, not within the layer, but at its interface with the neighboring stable stratum.

Physicists, too, have struggled with problems in which many scales interact simultaneously (cf. Wilson, 1979), but it is not known whether their renormalization group methods can be usefully applied to atmospheric or oceanic problems.

18.4.2 Natural Oscillations of the Atmosphere and Oceans

The quasi-geostrophic equations have been derived for ranges of the various nondimensional parameters that are of interest in dealing with particular classes of atmospheric and oceanic motions. It is not to be expected that they will remain uniformly valid throughout the entire range of rotationally dominated flows, even when the primary balance is geostrophic. Burger (1958) was the first to point out explicitly that when the β -plane approximation $L/a \ll 1$, where L is the characteristic horizontal scale and a is the radius of the earth, is no longer valid, the dynamics of the motion change radically. On a planetary scale the motion becomes even more strongly geostrophic, but the vorticity balance changes. Sverdrup (1947) made implicit use of this dynamics in his treatment of the steady, wind-driven circulation of the oceans, and it has been used for the treatment of steady thermohaline circulations of the oceans by Robinson and Stommel (1959) and Welander (1959). [See the review articles by Veronis (1969, 1973b), and chapter 5.]

In this section we present a classification of natural oscillations in atmospheres and oceans in which rotation plays a dominant role, paying special attention to the domain of validity of the β -plane, quasi-geostrophic equations, the nature of the oscillations for which these equations are not valid, and the effects of nonlinearity, which, especially in the oceans, may give rise to solitary wave behavior.

Although the wave forcing is very different in the oceans and the atmosphere, there are many features of the responses that strongly resemble one another. This results because the response of a forced system depends strongly on the characteristics of the natural oscillations, and these have many similarities in the atmosphere and oceans. We shall discuss both the linear and nonlinear natural (unforced and nondissipative) oscillations of a simple model consisting of a single-layer, homogeneous, incompressible fluid with a free surface on a β -plane. This is a much oversimplified model, and we must regard the conclusions to be drawn merely as

suggestions of the way in which the fully stratified, spherical system would behave. The most interesting implication—that the dynamics of scales intermediate between the Rossby radius and the radius of the earth may be dominated by solitary waves, in which nonlinear density advection balances linear dispersive effects—may not be very sensitive to the particular model chosen.

At the beginning of each subsection to follow we shall describe briefly the methods used and the results obtained in order to make it possible for the reader to omit the more detailed derivations. We begin the discussion of the normal modes of oscillation by stating the shallow-water equations in a reference frame moving with the wave. The Bernoulli and potential vorticity integrals then give two equations relating the wave streamfunction ϕ to the surface elevation η above the mean level H . These equations contain an unknown functional \mathcal{B} , the Bernoulli function, which we choose by requiring the equations to hold for vanishing ϕ and η .

We then obtain two coupled nonlinear partial differential equations defining an eigenvalue problem for the phase speed c . These equations have three nondimensional parameters: ϵ , a Rossby number measuring the ratio of the inertial to the Coriolis forces; \mathcal{S} , a static stability parameter measuring the ratio of the deformation scale L_R to the wave scale L ; and $\hat{\beta}$, the fractional change in the Coriolis parameter over the wave scale. In the standard quasi-geostrophic range ($\epsilon \sim \hat{\beta} \ll 1$, $\mathcal{S} \sim 1$), when motions have small Rossby numbers, length scales comparable to the deformation radius, the Bernoulli equation to lowest order is simply a statement of geostrophic balance, and the potential vorticity equation becomes the linear quasi-geostrophic wave equation.

The single-layer equations will be written in dimensional form

$$\begin{aligned} \frac{Du}{Dt} - (f_0 + \beta y)v &= -g\eta_x, \\ \frac{Dv}{Dt} + (f_0 + \beta y)u &= -g\eta_y, \\ \frac{D\eta}{Dt} + (H + \eta)(u_x + v_y) &= 0, \\ \frac{D}{Dt} &= \frac{\partial}{\partial t} + u \frac{\partial}{\partial x} + v \frac{\partial}{\partial y}, \end{aligned} \quad (18.1)$$

where η is the displacement of the surface from mean sea level, H is the mean depth of the fluid, g is the gravitational acceleration (we shall use a reduced gravity value here), $f_0 = 2\Omega \sin \Theta$, $\beta = 2\Omega \cos \Theta/a$, $y = a \Delta\Theta$, where Θ is the central latitude and $\Delta\Theta$ is the angular distance from Θ . In nondimensional form these equations become

$$\begin{aligned} \hat{\beta} \mathcal{S} \frac{Du}{Dt} - (1 + \hat{\beta}y)v &= -\eta_x, \\ \hat{\beta} \mathcal{S} \frac{Dv}{Dt} + (1 + \hat{\beta}y)u &= -\eta_y, \\ \hat{\beta} \frac{D\eta}{Dt} + (1 + \frac{\epsilon}{\mathcal{S}} \eta)(u_x + v_y) &= 0, \\ \frac{D}{Dt} &= \frac{\partial}{\partial t} + \frac{\epsilon}{\hat{\beta} \mathcal{S}} \left(u \frac{\partial}{\partial x} + v \frac{\partial}{\partial y} \right), \end{aligned} \quad (18.2)$$

where both x and y are scaled by L , η is scaled geostrophically by LUf_0/g , and the nondimensional parameters are $\hat{\beta} = \beta L/f_0 = L \cot \Theta/a \equiv L/L_\beta$, $\epsilon = U/f_0 L$, and $\mathcal{S} = gH/f_0^2 L^2 \equiv L_R^2/L^2$. We have also introduced the definitions of two scales which turn out to be important in determining the boundaries between various types of behavior: the β -scale $L_\beta = f_0/\beta = a \tan \Theta$, at which variations in the vertical component of the earth's angular velocity are order of the angular velocity itself, and the Rossby radius of deformation $L_R = \sqrt{gH}/f_0$ (Rossby, 1938). We shall use 3500 km for L_β (corresponding to $\Theta \sim 30^\circ$) and 50 km (oceanic) or 1000 km (atmospheric) for L_R . We have also made the choice of the long-wave period for the time scale so that $T = L/\beta L_R^2$.

The quasi-geostrophic potential vorticity equation may be derived by expanding (18.2) in powers of ϵ for $\hat{\beta} \sim \epsilon \ll 1$ and $\mathcal{S} \sim 1$, giving

$$\begin{aligned} \left[\frac{\partial}{\partial t} + \frac{\epsilon}{\hat{\beta} \mathcal{S}} \left(\eta_x \frac{\partial}{\partial y} - \eta_y \frac{\partial}{\partial x} \right) \right] \left(\nabla^2 \eta - \frac{1}{\mathcal{S}} \eta + \hat{\beta} y / \epsilon \right) \\ = 0. \end{aligned} \quad (18.3)$$

The failure of this equation at small space or time scales and near the equator is well known. Meteorologists since Burger (1958) have also recognized that some larger than synoptic-scale motions also do not evolve according to this equation. Rather, the appropriate equations are derived by assuming \mathcal{S} and ϵ to be small (because L is very large) and $\hat{\beta}$ to be of order 1. The resulting velocities remain geostrophic:

$$u = -\frac{1}{1 + \hat{\beta}y} \eta_y, \quad v = \frac{1}{1 + \hat{\beta}y} \eta_x, \quad (18.4)$$

and the height field evolves according to

$$\frac{\partial}{\partial t} \eta - \frac{1}{(1 + \hat{\beta}y)^2} \left(1 + \frac{\epsilon}{\mathcal{S}} \eta \right) \eta_x = 0. \quad (18.5)$$

Equations (18.3) and (18.5) have very different properties: the quasi-geostrophic equation has uniformly propagating linear-wave solutions which are essentially dispersive even at large amplitudes (cf. McWilliams and Flierl, 1979), while the Burger equation does not have uniformly propagating linear-wave solutions and initial disturbances steepen because of non-

linearity. We shall demonstrate that there is an intermediate band of length scales in which nonlinearity and dispersion can balance to give cnoidal or solitary waves. In the ocean, as we shall see, the change from quasi-geostrophic to intermediate dynamics to Burger dynamics occurs at a relatively small scale because the deformation radius is so small compared to the radius of the earth.

We may elucidate these differences by considering the shallow-water equations under the assumption that the motions are translating steadily at speed c :

$$\begin{aligned} (\mathbf{v} - c\hat{\mathbf{x}}) \cdot \nabla \mathbf{v} + \hat{\mathbf{z}}(f_0 + \beta y) \times \mathbf{v} &= -g \nabla \eta, \\ (\mathbf{v} - c\hat{\mathbf{x}}) \cdot \nabla \eta + (H + \eta) \nabla \cdot \mathbf{v} &= 0, \end{aligned} \quad (18.6)$$

where $\hat{\mathbf{x}}$ and $\hat{\mathbf{z}}$ are unit vectors in the positive x and z directions. We may define a transport streamfunction in the coordinate system moving with the wave

$$(\mathbf{v} - c\hat{\mathbf{x}})(H + \eta) = \hat{\mathbf{z}} \times \nabla \psi$$

and write the Bernoulli and potential vorticity integrals of motion:

$$\begin{aligned} \frac{1}{2} |\nabla(\phi + cHy)|^2 + g(H + \eta)^3 + c(H + \eta)^2 \left(f_0 y + \frac{\beta y^2}{2} \right) \\ = (H + \eta)^2 \mathcal{B}(\phi + cHy), \end{aligned} \quad (18.7)$$

$$\nabla \cdot \frac{\nabla(\phi + cHy)}{H + \eta} + (f_0 + \beta y) = (H + \eta) \mathcal{B}'(\phi + cHy),$$

where we have isolated the wave part of the streamfunction $\phi = \psi - cHy$. We require that (18.7) hold as $\phi, \eta \rightarrow 0$; this determines the Bernoulli functional

$$\mathcal{B}(Z) = \frac{c^2}{2} + gH + \frac{f_0}{H} Z + \frac{\beta}{2cH^2} Z^2. \quad (18.8)$$

The choice of a single-valued, well-behaved Bernoulli functional implies that only motions which reduce smoothly to linear waves will be considered; thus the solutions of Stern (1975b) or Flierl, Larichev, McWilliams, and Reznik, (1980) which involve closed streamlines and a multiple-valued \mathcal{B} will not be examined here.

In nondimensional form, equations (18.7) become

$$\begin{aligned} \frac{\epsilon}{2} |\nabla \phi|^2 + \hat{S} \hat{S} c \phi_\nu + \eta \left(1 + \frac{\epsilon}{\hat{S}} \eta \right) \\ = \hat{S}^2 \hat{S} c^2 \eta \left(1 + \frac{\epsilon}{2\hat{S}} \eta \right) + \phi \left(1 + \hat{\beta} y \right) \left(1 + \frac{\epsilon}{\hat{S}} \eta \right)^2 \\ + \frac{\epsilon}{\hat{S}} \frac{\phi^2}{2c} \left(1 + \frac{\epsilon}{\hat{S}} \eta \right)^2, \end{aligned} \quad (18.9)$$

$$\begin{aligned} \hat{S} \nabla^2 \phi \left(1 + \frac{\epsilon}{\hat{S}} \eta \right) - \epsilon \nabla \phi \cdot \nabla \eta - \hat{\beta} \hat{S} c \eta_\nu \\ = \eta \left(1 + \hat{\beta} y \right) \times \left(1 + \frac{\epsilon}{\hat{S}} \eta \right)^2 + \frac{\phi}{c} \left(1 + \frac{\epsilon}{\hat{S}} \eta \right)^3. \end{aligned} \quad (18.10)$$

We show in figure 18.1 the dependence upon L and U of our three basic parameters $\hat{\beta} = L/L_\beta = \beta L/f_0 = L \cot \Theta/a$ (the ratio of the wave scale to the radius of the earth scale), $\epsilon = U/f_0 L$ (the Rossby number), and $\hat{S} = L_R^2/L^2$ (the inverse of the rotational Froude number). Note immediately the differences in scale separation for oceanic versus atmospheric conditions. In the atmosphere L_β is very close to L_R , so that there is only a short range between the usual baroclinic Rossby wave scales ($\hat{S} \sim 1, \beta \ll 1$) and the Burger range ($\hat{S} \ll 1, \hat{\beta} \sim 1$); in the ocean there is a large scale gap. Thus one might expect the different dynamics to be seen more clearly in the ocean.

Linear Waves ($\epsilon = 0$) The first step toward understanding the various types of large-scale free motion is to consider the linearized solutions. When the Rossby number is very small, the two equations can be combined into a single streamfunction equation which governs both gravity and Rossby waves. The Rossby wave-phase speed increases as the length scales of the wave increase, leveling off for $L > L_R$. For still larger scales, however, the speed again increases as the wave amplitude begins to be more pronounced equatorially. We demonstrate that the natural dividing scale here is what we call the "intermediate" scale $L_1 \equiv (L_\beta L_R^2)^{1/3}$, where $\hat{S} = \hat{\beta}$ (see figure 18.1). This is the scale at which

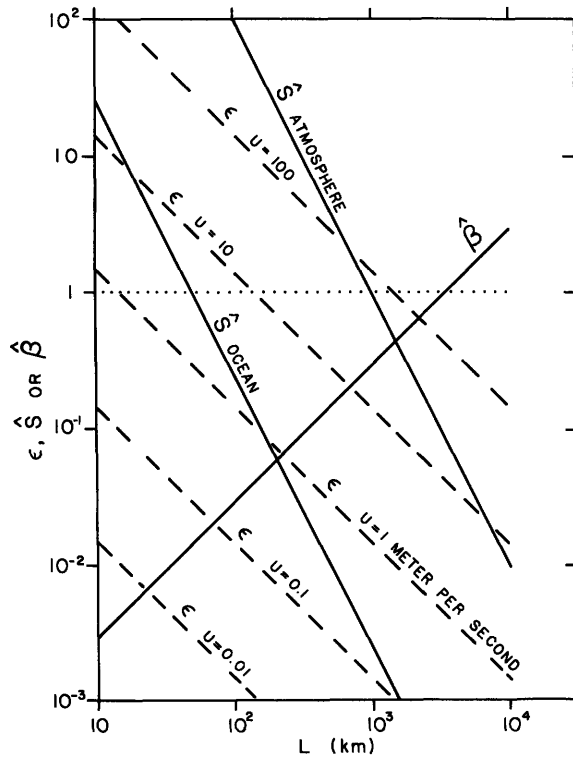


Figure 18.1 Values of the Rossby number ϵ , inverse Froude number \hat{S} , and beta parameter $\hat{\beta}$ as functions of the length scale L and velocity scale U for oceanic and atmospheric values of the deformation radius.

the relative vorticity changes become as small as the variations in vortex stretching due to the β term. Alternatively, one could say that the rule, “ f equals a constant except when differentiated,” breaks down near the intermediate scale. The phase speed continues to increase and, for large enough north-south scales, the wave domain crosses the equator. Then the wave becomes equatorially trapped and the phase speed again becomes independent of L .

For the parameters we have chosen— $L_\beta = 3500$ km, $L_R = 50$ km (ocean), 1000 km (atmosphere)—the intermediate scale $L_I = 210$ km (ocean), 1500 km (atmosphere) is not very large. It represents the upper bound to the scales for which the standard quasigeostrophic equations are valid. It may again be seen that there is a significantly greater separation among the various scales in the ocean compared to the atmosphere. This suggests that the ocean mesoscale motions may be a cleaner example of quasi-geostrophic flow than the synoptic-scale motions of the atmosphere; the approximations used for the latter are less exact.

For linear motions, the Bernoulli equation (18.9) defines η in terms of ϕ ; η may then be eliminated from the potential vorticity equation (18.10) to yield a single equation for the streamfunction

$$\hat{S} \nabla^2 \phi - \frac{1}{c} \phi - (1 + \hat{\beta}y)^2 \phi = \hat{\beta}^2 \hat{S}^2 c^2 \phi_{xx}. \quad (18.11)$$

Since the coefficients do not involve x , we may set $\phi = e^{ix}G(y;L)$. The resulting equation together with boundary conditions presents an eigenvalue problem for $c(L)$ and the wave structure $G(y;L)$.

It has three eigenvalues, corresponding to two gravity-wave modes and one Rossby-wave mode. We can identify the gravity modes with the retention of the right-hand term in (18.11). For mid-latitude modes this term is significant only when $\hat{\beta}^2 \hat{S}^2 c^2 \sim \hat{S}$ or c^2 (dimensional) $\sim gH$; it is small for the Rossby mode solutions. For equatorially trapped Rossby modes, the y scale contracts so that $\hat{S} \phi_{yy}$ dominates both $\hat{S} \phi_{xx}$ and $\hat{\beta}^2 \hat{S}^2 c^2 \phi_{xx}$. Eliminating the right-hand side corresponds to retaining only the underlined terms in (18.9)–(18.10). The filtered linear equation becomes

$$\hat{S} \nabla^2 \phi - \frac{1}{c} \phi = (1 + \hat{\beta}y)^2 \phi, \quad (18.12)$$

which has been discussed extensively by Lindzen (1967) and others. Here we comment on the various types of solution primarily as a guide to our later discussion of the effects of nonlinearity.

Figure 18.2 shows the nondimensional phase speed as a function of L for atmospheric or oceanic parameters under the simplifying boundary conditions $\phi = 0$ at $y = \pm\pi/2$, which make the x and y scales of the

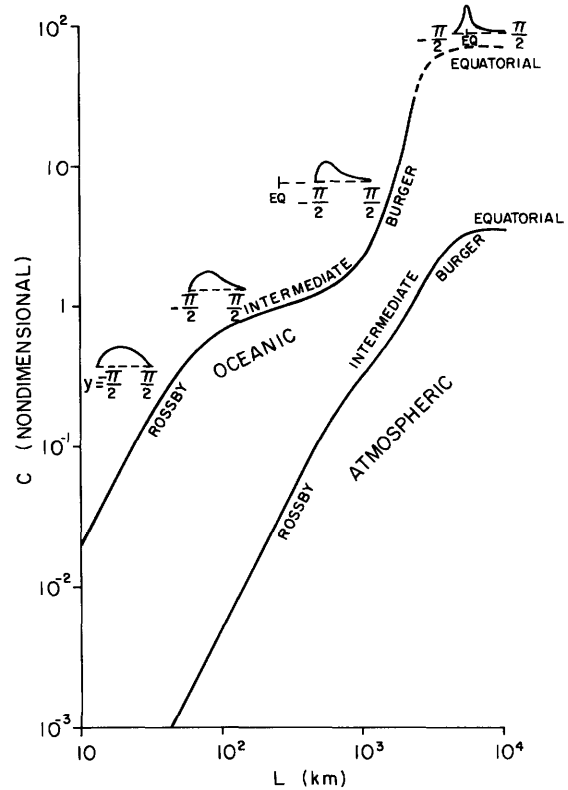


Figure 18.2 Phase speed nondimensionalized by βL_R^2 as a function of the x scale L (wavelength/ 2π) in a channel of width πL . Also shown are typical shapes of the y structure function $G(y;L)$ for the various classes of motion.

domain similar. We can identify four different types of behavior.

Midlatitude Rossby waves ($\hat{\beta} \ll 1$, $\hat{S} \sim 1$): For these motions, first described by Rossby et al. (1939), the streamfunction satisfies

$$\hat{S} \nabla^2 \phi - \frac{1}{c} \phi = \phi, \quad (18.13)$$

which has solutions in the box

$$\phi = e^{ix} \cos y$$

with

$$c = -1/(1 + 2\hat{S}), \quad (18.14)$$

or, more generally, for waves oriented in any direction, we have

$$\phi = e^{i\mathbf{k}\cdot\mathbf{x}}$$

with

$$c = -1/(1 + \hat{S} \mathbf{k}\cdot\mathbf{k}) \quad (18.15)$$

(see the discussion in chapter 10).

Intermediate scale waves ($\hat{\beta} \sim \hat{S} \ll 1$): The Rossby-wave dispersion relation (18.14) remains valid for $\hat{\beta} \ll \hat{S} \ll 1$ and becomes

$$c = -1 + 2\hat{S},$$

so that for a sufficiently small \hat{S} the waves are nondispersive c (dimensional) $= -\beta L_R^2$. However, when L increases to the point where $\beta \sim \hat{S} \ll 1$, the small correction in the formula above becomes invalid. This occurs when the $\phi\hat{\beta}y$ term becomes comparable to the $\hat{S}\nabla^2\phi$ term, that is, when $L \approx [L_\beta L_R^2]^{1/3}$, which is 210 km for the oceans or 1500 km for the atmosphere. We denote this scale as the "intermediate scale" L_I . The wave structure is determined by expanding (18.12) in \hat{S} (or $\hat{\beta}$). Setting $\phi = \phi^{(0)} + \hat{S}\phi^{(1)} + \dots$ and $c = -1 + \hat{S}c^{(1)} + \dots$, we obtain

$$(\nabla^2 + c^{(1)} - 2\hat{\beta}y/\hat{S})\phi^{(0)} = 0. \quad (18.16)$$

When $L \geq L_I$ the y dependence of f can no longer be neglected, the y scale becomes order of the intermediate scale, and the solutions begin to be concentrated toward the equator (see figure 18.2). As L continues to increase, \hat{S} decreases but $\hat{\beta}$ increases and the phase speed is no longer insensitive to L but begins to increase; c behaves like $-1 + O(\hat{\beta})$ rather than $-1 + O(\hat{S})$. The phase speed becomes less and less sensitive to the x wavenumber, so that the waves may still be considered approximately nondispersive. We have required that $\hat{\beta}$ and \hat{S} be small, but figure 18.1 shows that these quantities are small only for a rather narrow range of L even in the oceanic case, and figure 18.2 shows that c varies perceptibly with L everywhere. For the atmospheric parameters a totally nondispersive regime ($\hat{\beta} \ll \hat{S} \ll 1$) does not exist at all.

Burger motions ($\hat{\beta} \sim 1, \hat{S} \ll 1$): When L increases to the point where $\hat{\beta} \sim 1$, the motions become strongly concentrated near the equator. The y scale contracts (relative to L) so that the lowest order balance includes all the terms in (18.12) and the y wave domain crosses the equator. The phase speed rapidly increases from that of the midlatitude Rossby waves to that of the equatorial waves.

Now we can see why the Burger equation (18.5), which assumes equal x and y scales, has no linear free-wave solutions: free waves with a very large x scale do not have the same y scale. Instead the unforced motions acquire a meridional scale between L_I and the (somewhat larger) equatorial scale. Forced motions, of course, may have comparable x and y scales and may therefore have evolution equations in which the terms of (18.5) contribute along with the forcing terms.

Equatorial waves: Here we can drop the 1 in the $1 + \hat{\beta}y$ term of equation (18.12) to change to the equatorial β -plane (the f_0 factors will all cancel out upon dimensionalization). The solutions are well known (cf. Lindzen, 1967) and again become nondispersive for small \hat{S} . Rescaling the equation for small \hat{S} shows that the y wave domain is confined to a region around the equator of meridional extent $\hat{\beta}^{-1/2}\hat{S}^{1/4}$, which corresponds to the

dimensional scale $L_e = [gH/\beta^2]^{1/4} = [L_\beta L_R]^{1/2}$, the well-known equatorial deformation scale. For our assumed parameters, this scale is 420 km for the oceans and 1900 km for the atmosphere; however, this estimate is not very accurate since the equivalent depth for baroclinic motions varies considerably. Moore and Philander (1977) give 325 km as an estimate of this scale for the first baroclinic mode. The phase speeds are order $\hat{\beta}^{-1}\hat{S}^{-1/2} = L_\beta/L_R$, corresponding to a dimensional speed $\beta L_e^2 = \sqrt{gH}$. (The other solutions have $c \sim \pm\hat{\beta}^{-1/2}\hat{S}^{-3/4}$.) A further discussion appears in chapter 6.

Nonlinear Waves ($\epsilon > 0$) When the motion becomes of sufficiently large amplitude, the propagation characteristics of a single wave change. We shall investigate the size of the Rossby number necessary for this to occur. This size may be quite different from the Rossby number required for significant nonlinear interactions in a full spectrum of waves. However, the nonlinear behavior of a single wave can be of interest when it allows the possibility for solitary waves. On the scale of the mid-latitude Rossby wave, this does not appear to occur and the nonlinearity gives only a correction to the phase speed and shape; the lowest-order balance remains strongly dispersive. However, as the scale becomes equal to or greater than the intermediate scale, the phase speed becomes less dependent on the x wavenumber. When the Rossby number becomes of the order L_R^4/L^4 , the nonlinear advection term becomes comparable to the east-west dispersion term and the solutions propagate as solitary waves. The structure of these isolated high-pressure disturbances is found to be the same as that of the sech^2x solution to the Korteweg-deVries equations. The implication of this section, then, is that the dynamics of motions of the intermediate or large scales may be quite different from that of the ordinary Rossby wave.

Let us now consider the conditions under which the nonlinear terms can alter the propagation characteristics of the free waves in our model. This can occur whenever one of the ϵ terms is comparable to one of the linear terms that have been retained in the Bernoulli or potential vorticity equations (18.9)–(18.10) (the underlined terms). This happens when $\epsilon \sim 1$, $\epsilon/\hat{\beta} \sim 1$, $\epsilon/\hat{S} \sim 1$, $\epsilon/\hat{\beta}\hat{S} \sim 1$, or $\epsilon/\hat{S}^2 \sim 1$. The velocities required for each of these conditions are shown in figure 18.3, which emphasizes again the relative complexity of the atmosphere: for 40- ms^{-1} winds at 1000-km scales, all of the nonlinear terms enter simultaneously. For the ocean, only strong meandering motions could cause each of ϵ , ϵ/\hat{S} and ϵ/\hat{S}^2 to be of order unity, and in these circumstances $\hat{\beta}$ remains quite small. We shall not attempt to deal with these more complicated motions, but instead shall examine the nonlinear ef-

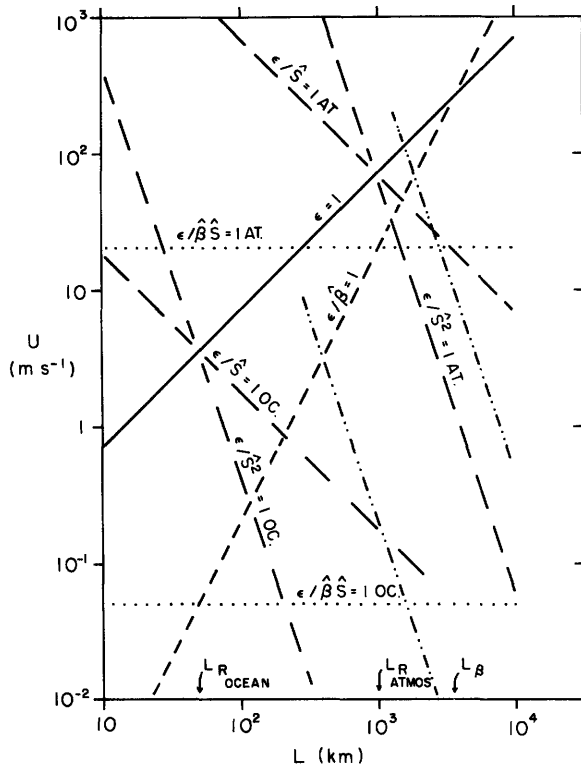


Figure 18.3 Conditions under which nonlinear terms become important. Labeled curves show relationship between U and L such that a particular parameter ratio becomes equal to one. This corresponds to one of the nonlinear terms in (18.9)–(18.10) becoming equal in magnitude to one of the underlined linear terms.

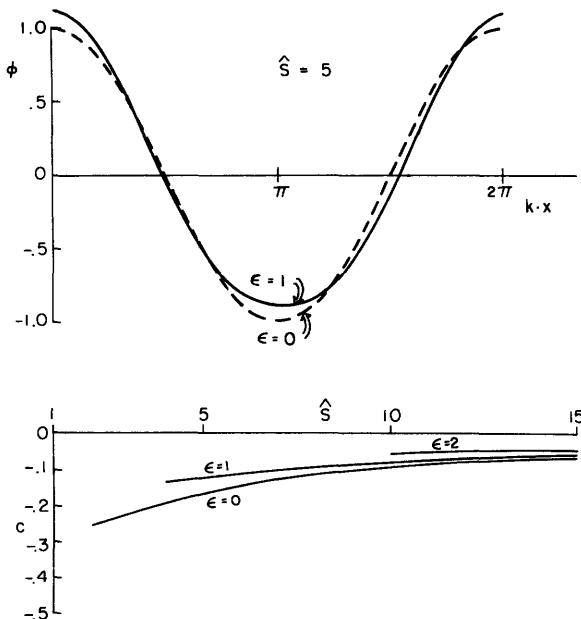


Figure 18.4 Effects of nonlinearity on a short Rossby wave. The upper figure shows the changes in the shape of the wave. The lower figure shows the changes in the dispersion relation.

fects on each of the waves that has been considered above.

Midlatitude Rossby waves: The first nonlinear condition that occurs when $\hat{S} \geq 1$ is $\epsilon = \hat{\beta}$. However, since $\hat{\beta}$ remains small and does not enter the governing equation (18.13), we expect that this will not significantly alter the behavior of a single steadily propagating sinusoidal wave. When ϵ or ϵ/\hat{S} becomes order 1, nonlinearity begins to affect the structure significantly. For example, consider the parameter range $\epsilon \sim 1$, $\hat{\beta} \ll \hat{S}^{-1} \ll 1$. To lowest order in an expansion of both ϕ and c in \hat{S}^{-1} (c being of order \hat{S}^{-1}), the potential vorticity equation gives

$$\nabla^2 \phi^{(0)} = \frac{1}{c^{(0)\hat{S}}} \phi^{(0)}.$$

At first order we find the corrections to the phase speed and shape of the wave. The result is

$$c = \hat{S}^{-1} \left[-\frac{1}{\mathbf{k} \cdot \mathbf{k}} + \hat{S}^{-1} \left(\epsilon^2 + \frac{1}{(\mathbf{k} \cdot \mathbf{k})^2} \right) + \dots \right], \quad (18.17)$$

as sketched in figure 18.4. The order ϵ nonlinear terms cause a sharpening of the streamfunction crests and a decrease in the propagation rate.

Intermediate scale waves: When $\hat{S} \ll 1$, nonlinear terms first enter when $\epsilon \sim \hat{\beta}\hat{S}$ or $\epsilon \sim \hat{S}^2$ (see figure 18.3). We can find the forms of the solutions by letting $\epsilon = E\hat{S}^2$ and $\hat{\beta} = B\hat{S}$ and expanding for small \hat{S} assuming E , B to be of order unity or less. We get

$$c = -1 + \hat{S}c^{(1)}, \quad (18.18)$$

$$\nabla^2 \phi^{(0)} + c^{(1)}\phi^{(0)} + \frac{3}{2}E[\phi^{(0)}]^2 - 2By\phi^{(0)} = 0$$

for the equations governing the shape and the speed of the wave.

The simple limit here is $B = \hat{\beta}/\hat{S} \ll 1$, corresponding to the range $L_R \ll L \ll L_I$, and E of order unity, corresponding to particle speeds given by the $\epsilon/\hat{S}^2 = 1$ lines in figure 18.3. The wave equation

$$\nabla^2 \phi^{(0)} + c^{(1)}\phi^{(0)} + \frac{3}{2}E[\phi^{(0)}]^2 = 0$$

has both one- and two-dimensional solutions on the plane. These include the cnoidal and solitary wave solutions to the Korteweg–deVries equation (Whitham, 1974) for uniformly propagating waves:

$$\phi^{(0)} = cn^2 \left(\frac{K(m)}{\pi} \frac{\mathbf{k} \cdot \mathbf{x}}{|\mathbf{k}|}; m \right) - \frac{\sqrt{1-m+m^2}-1+2m}{3m},$$

$$c = -1 + \hat{S}4K^2(m)\sqrt{1-m+m^2}/\pi^2, \quad (18.19a)$$

$$\epsilon\hat{S}^{-2} = 4mK^2(m)/\pi^2,$$

and

$$\begin{aligned} \phi^{(0)} &= \text{sech}^2 \mathbf{k} \cdot \mathbf{x}, \\ c &= -1 - 4\hat{S}\mathbf{k} \cdot \mathbf{k}, \\ \epsilon \hat{S}^{-2} &= 4\mathbf{k} \cdot \mathbf{k}. \end{aligned} \quad (18.19b)$$

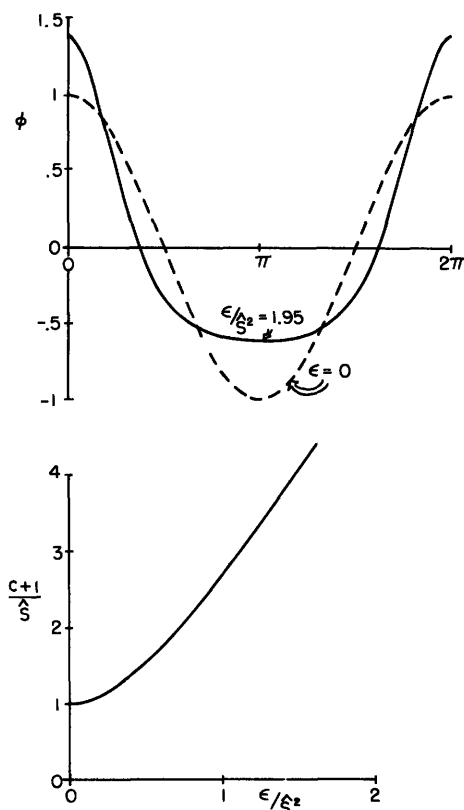
Plots of the shapes of the cnoidal and solitary waves and the dispersion relations are shown in figures 18.5A and 18.5B. The cnoidal waves show a phase speed decreasing with amplitude (as in the example above) while the solitary wave speed increases as the wave gets stronger.³

A second type of solution (cf. Flierl, 1979b) is a radially symmetric solitary wave

$$\begin{aligned} \phi^{(0)} &= G(k\sqrt{\mathbf{x} \cdot \mathbf{x}}), \\ c &= -1 - \hat{S}k^2, \\ \epsilon \hat{S}^{-2} &= 1.59k^2, \end{aligned} \quad (18.19c)$$

whose shape and dispersion relations are shown in figure 18.6.

It may be seen from equation (18.15) that the dynamics of large-scale motions for which $\epsilon \sim \hat{S}^2$ and $\hat{\beta} \ll \epsilon/\hat{S}$ are distinctly different from those of the quasigeo-

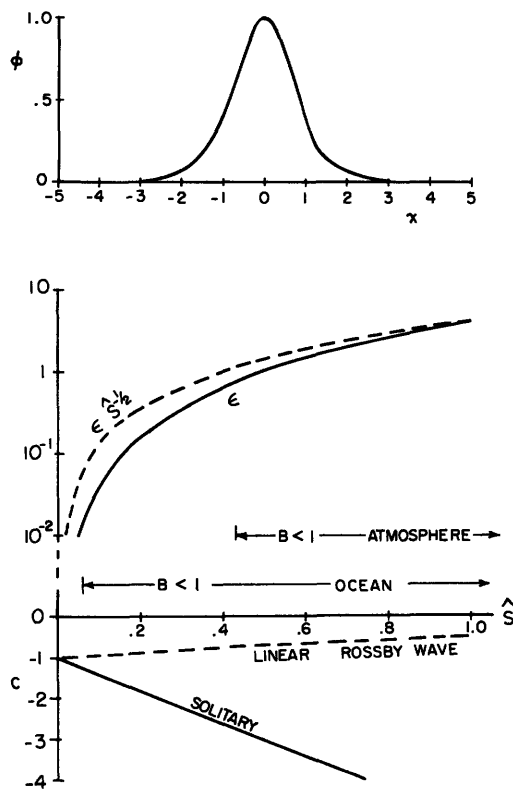


18.5(A)

Figure 18.5 Effects of nonlinearity on long waves. (A) Cnoidal waves: the upper figure shows the change in shape occurring when the nonlinearity is increased while the lower figure shows the changes in the dispersion relation. (B) Solitary waves: the upper figure shows the shape of the wave while

strophic eddies. We might expect, if the motions are governed by the Korteweg–deVries equation as suggested by (18.18), that solitons will be formed and dominate the subsequent evolution of the field. In the atmosphere, solitary-wave behavior would be difficult to find because of the rapid frictional decay time, the east–west periodicity for scales not so much larger than those under consideration, and the rather limited parameter range for the Korteweg–deVries regime. In the ocean, the situation is quite different; the parameter range for solitary-wave behavior is more distinct, the waves are of small scale compared to the size of the basin, and the decay rates are slow so that there is sufficient space and time for the necessary balance between nonlinearity and dispersion to develop.

For scales larger than the intermediate scale, B becomes large in (18.18). If y is rescaled by $B^{-1/3}$ (dimensionally by L_1), this equation can be solved by expansion in powers of $B^{-2/3}$. To lowest order, one obtains a linear equation for the y structure; to next order, the x dispersion and nonlinear steepening (if E is order unity) are included and the x structure is then given by an equation of the Korteweg–deVries type.



18.5(B)

the lower figure shows the relationship between the length and amplitude (\hat{S} and ϵ) and also the propagation speed. For a fixed deformation radius, $\epsilon \hat{S}^{-1/2}$ is directly proportional to the velocity scale U . The relationships are only valid for $B < 1$.

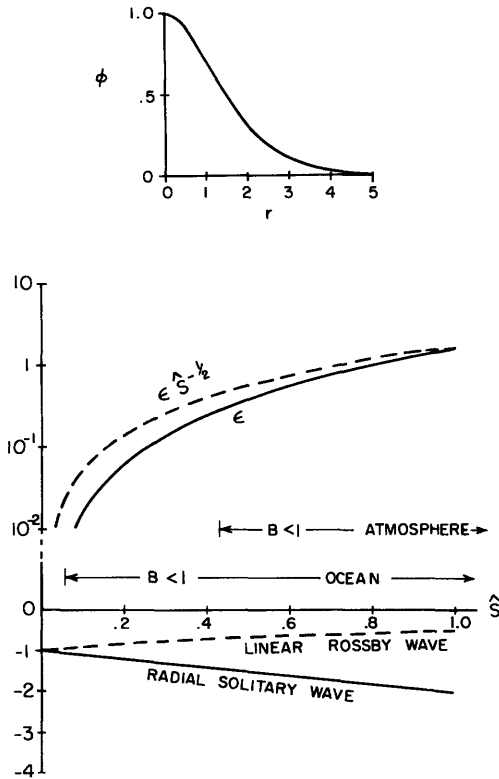


Figure 18.6 Radially symmetric solitary solutions. The upper figure shows the dependence of the pressure upon radius. The lower figure gives the relationships between amplitude, size, and propagation speed.

Burger range: Here also one can show that there are motions whose y structure is determined by a linear equation and whose x structure is determined by a nonlinear equation of the Korteweg–deVries type. We still require $\epsilon \sim \hat{S}^2$. Clarke (1971) has discussed this type of solution (and also those described above for large B) in more detail.

Equatorial motions: Boyd (1977) has shown that the long waves in this case also satisfy an equation of the Korteweg–deVries type. If we rescale the equatorial versions of (18.9) and (18.10), letting $y = \hat{\beta}^{-1/2} \hat{S}^{1/4} Y$ (so that Y has the scale L_e), $c = \hat{\beta}^{-1} \hat{S}^{-1/2} C$, and $\eta = \hat{\beta}^{1/2} \hat{S}^{1/4} N$, we can show that there are only two parameters (in the absence of north–south boundaries) of interest: $\delta = \hat{\beta}^{-1/2} \hat{S}^{1/4} = L_e/L$ and $\hat{\epsilon} = \epsilon \hat{\beta}^{1/2} \hat{S}^{-3/4} = UL/\beta L^3$. The cnoidal or solitary wave (in x) solutions are obtained when $\hat{\epsilon} \sim \delta^2 \ll 1$. This gives an equatorial velocity scale $U = \beta L_e^2/L^3$, as shown in figure 18.3.

In summary, then, we have seen three different types of natural large-scale, long-period motions in the atmosphere and ocean. For scales on the order of the deformation radius or less ($L \lesssim 50$ for the oceans and $\lesssim 1000$ km for the atmosphere), dispersive Rossby waves dominate with nonlinear effects entering only for large Rossby number ϵ . Intermediate scales ($\hat{S} \ll 1$, $\epsilon \hat{S}^{-2} \sim 1$, $\hat{\beta} \ll \epsilon \hat{S}^{-1}$ implying $50 \ll L \ll 210$ km for

the oceans and $1000 \ll L \ll 1500$ km for the atmosphere) have solitary or cnoidal wave structures as well as circular solitary highs. As the scales become larger, weak solitary or cnoidal wave structures may persist with normal-mode y shapes concentrated near the equatorward side of the domain. Stronger motions will not remain permanent but will steepen in amplitude, as do the solutions of Burger’s equation (18.5). When the wave domain comes to include the equator, nonlinear equatorial wave motions satisfying a Korteweg–deVries type of equation can exist.

Korteweg–deVries Dynamics Finally we shall demonstrate that Korteweg–deVries dynamics does seem to be appropriate for general motions (not necessarily uniformly propagating waves) on the intermediate scale ($\hat{\beta} \geq \hat{S}$, $\epsilon \sim \hat{S}^2$, and $\hat{S} \ll 1$). The previous derivations have shown only that the permanent form is governed by an equation that may be derived from the Korteweg–deVries equation, but it is still necessary to show that the time-dependent evolution equation is also of this type. We return to our governing equations (18.2) and set $\epsilon = E \hat{S}^2$ and $\hat{\beta} = B \hat{S}$, where B and E are assumed to be of order unity. This corresponds to $L \sim L_1$ and $U \sim f_0 L_R^2/L_\beta$ (210 km, 5 cm s⁻¹ for the ocean; 1500 km, 20 m s⁻¹ for the atmosphere). We note that there will be two time scales in the evolution: a fast time t corresponding to the nondispersive propagation and a slow time $T = \hat{S}t$ during which features evolve.

The lowest two orders of the expansion in \hat{S} show that the flow is geostrophic and that the advection of planetary vorticity is balanced by vortex stretching, leading to the usual nondispersive propagation of very long Rossby waves. At the next order slow changes in surface height force a divergence which creates relative vorticity. The vorticity balance also is influenced by north–south variations in vortex stretching due to variations of f , while the nonlinear terms enter in the mass balance. The resulting equation is a mix between the Korteweg–deVries equation and the Rossby-wave equation. However, when L is large compared to the intermediate scale, the more detailed expansion to follow shows that the x structure indeed evolves according to a Korteweg–deVries equation.

At lowest order the flows are geostrophic

$$u^{(0)} = -\eta_y^{(0)},$$

$$v^{(0)} = \eta_x^{(0)},$$

$$u_x^{(0)} + v_y^{(0)} = 0.$$

The first-order equations,

$$u^{(1)} + B y u^{(0)} = -\eta_y^{(1)},$$

$$v^{(1)} + B y v^{(0)} = \eta_x^{(1)},$$

$$B \eta^{(0)} + E v^{(0)} \cdot \nabla \eta^{(0)} + E \eta^{(0)} \nabla \cdot v^{(0)} + \nabla \cdot v^{(1)} = 0,$$

lead to Sverdrup (1947) or Burger (1958) type of balance between advection of planetary vorticity and vortex stretching,

$$u_x^{(1)} + v_y^{(1)} = -B\eta_x^{(0)},$$

and to the nondispersive wave equation

$$B\eta_t^{(0)} - B\eta_x^{(0)} = 0,$$

which implies

$$\frac{\partial}{\partial t} = \frac{\partial}{\partial x} \quad \text{or} \quad \eta = \eta(x + t, y, T).$$

At second order we obtain the vorticity equation

$$B(v_x^{(0)} - u_y^{(0)}) + E\mathbf{v}^{(0)} \cdot \nabla(v_x^{(0)} - u_y^{(0)}) \\ + Bv^{(1)} + \nabla \cdot \mathbf{v}^{(2)} - By \nabla \cdot \mathbf{v}^{(1)} = 0$$

and the mass-conservation equation

$$B\eta_t^{(0)} + B\eta_t^{(1)} + E\mathbf{v}^{(1)} \cdot \nabla \eta^{(0)} + E\mathbf{v}^{(0)} \cdot \nabla \eta^{(1)} \\ + \nabla \cdot \mathbf{v}^{(2)} + E\eta^{(1)} \nabla \cdot \mathbf{v}^{(0)} + E\eta^{(0)} \nabla \cdot \mathbf{v}^{(1)} = 0,$$

which jointly lead to the evolution equation [after using $\partial/\partial t = \partial/\partial x$ for the fast time, and dropping the superscript (0)]

$$B\eta_T = EB\eta\eta_x + B(\nabla^2 \eta)_x \\ - 2B^2 y \eta_x + EJ(\eta, \nabla^2 \eta) \quad (18.20)$$

[where $J[A, B]$ is the Jacobian operator] or

$$B\eta_T = EJ(\eta - \frac{B}{E} y, \nabla^2 \eta + \frac{3}{2} E\eta^2 - 2By\eta).$$

One can readily show that the requirement of steady propagation leads to (18.18). Furthermore, when L is large compared to the intermediate scale L_I but E remains order one, the x structure of the solutions do satisfy a Korteweg–deVries equation. In this case B is large and E is order 1. Because the y scale becomes limited to L_I , the x dependence and the nonlinearity do not enter in the primary balance, which serves to determine the y structure and a correction to the phase speed. At the next order, the nonlinearity (from both quadratic and Jacobian terms) enters along with the third x derivative and the slow-time derivative terms to give a Korteweg–deVries equation:

$$\eta = F(x - ct, T)Ai(\mathcal{Y}), \\ c = -1 - \pi B - (2B)^{2/3}\mathcal{Y}_0, \\ \mathcal{Y} = \mathcal{Y}_0 + (2B)^{1/3} \left(y + \frac{\pi}{2} \right), \\ \mathcal{Y}_0 = -2.3381 \quad (\text{zero of Airy function}), \\ F_T = F_{xxx} + \frac{3}{2} E \left(\int_{\mathcal{Y}_0}^{\infty} Ai^3 / \int_{\mathcal{Y}_0}^{\infty} Ai^2 \right) \frac{\partial}{\partial x} F^2. \quad (18.21)$$

This section has demonstrated that some caution must be exercised in applying the quasi-geostrophic equations (which will be discussed throughout the rest of the paper) to large-scale motions since they are valid for the oceans only for scales up to the order of 200 km. The derivations suggest that the role of nonlinearity may be very different for the intermediate and large-scale motions—leading to coherent and phase-locked structures rather than to turbulence. Clearly these inferences must be backed up by more thorough investigations which are beyond the scope of this article.

18.4.3 The Quasi-Geostrophic Equations

Because of the difficulties inherent in attacking the full equations of motion either analytically or numerically, various approximative equations have been developed. For the study of the large-scale motions, the relevant “filtering approximations” eliminate the acoustic and inertigravity motions.⁴ We have mentioned the quasi-geostrophic, semigeostrophic and balance equations and have touched on their limitations. In this section we shall discuss briefly the derivation of the quasi-geostrophic equations for a stratified fluid under oceanic conditions; details can be found in the appendix. These equations are, of course, familiar, but, since we shall use them in the rest of this chapter, we must establish our notation. We wish also to remark on differences between the standard derivation for the atmosphere (cf. Charney, 1973) and that for oceanic conditions. Finally, we include the β -effect by explicitly taking into account the two-scale nature of the problem: the planetary scale, that is, the earth’s radius, and the scale of the fluid motions themselves.

For inviscid, adiabatic flow, the equations of motion and continuity expressed in modified spherical coordinates are

$$\frac{Du}{Dt} + \frac{uw}{a+z} - \frac{uv \tan \Theta}{a+z} - 2\Omega v \sin \Theta + 2\Omega w \cos \Theta \\ = -\frac{\alpha}{(a+z) \cos \Theta} \frac{\partial p}{\partial \Phi}, \\ \frac{Dv}{Dt} + \frac{wv}{a+z} + \frac{u^2 \tan \Theta}{a+z} + 2\Omega u \sin \Theta = -\frac{\alpha}{a+z} \frac{\partial p}{\partial \Theta}, \\ \frac{Dw}{Dt} - \frac{u^2 + v^2}{a+z} + 2\Omega u \cos \Theta = -\alpha \frac{\partial p}{\partial z} - g, \quad (18.22) \\ -\frac{1}{\alpha} \frac{D\alpha}{Dt} + \frac{1}{(a+z) \cos \Theta} \frac{\partial u}{\partial \Phi} + \frac{1}{(a+z) \cos \Theta} \frac{\partial}{\partial \Theta} (v \cos \Theta) \\ + \frac{1}{(a+z)^2} \frac{\partial}{\partial z} (a+z)^2 w = 0, \\ \frac{D}{Dt} = \frac{\partial}{\partial t} + \frac{u}{(a+z) \cos \Theta} \frac{\partial}{\partial \Phi} + \frac{v}{a+z} \frac{\partial}{\partial \Theta} + w \frac{\partial}{\partial z},$$

where Φ is the longitude, Θ the latitude, Ω the angular speed of the earth's rotation, g the acceleration of gravity, p the pressure, α the specific volume, and u, v, w the eastward, northward, upward velocity components, respectively. The radial coordinate is denoted by $a + z$, where a is the mean radius of the earth and z the height above mean sea level. This neglects the ellipticity of the geoid [see Veronis (1973b) for a discussion of this approximation].

We assume that the specific volume is determined by an equation of state as a function of absolute temperature T , salinity \mathcal{S} , and pressure:

$$\alpha = \alpha(T, \mathcal{S}, p) \quad (18.23)$$

with salinity conserved,

$$\frac{D}{Dt} \mathcal{S} = 0, \quad (18.24)$$

and temperature changes determined from the adiabatic thermodynamics

$$\frac{DT}{Dt} - \frac{T}{c_p} \left(\frac{\partial \alpha}{\partial T} \right)_{p, \mathcal{S}} \frac{Dp}{Dt} = 0. \quad (18.25)$$

For dynamical modeling it is convenient to regard temperature as a function of specific volume, salinity, and pressure and to determine the evolution of the specific volume from

$$\frac{D\alpha}{Dt} + \frac{\alpha^2}{c_s^2} \frac{Dp}{Dt} = 0, \quad (18.26)$$

which can be derived by taking the substantial derivative of (18.23), using (18.24)–(18.25) and the definition of the sound speed:

$$c_s^2 \equiv -\alpha^2 \left[\frac{T}{c_p} \left(\frac{\partial \alpha}{\partial T} \right)_{p, \mathcal{S}} + \left(\frac{\partial \alpha}{\partial p} \right)_{T, \mathcal{S}} \right]^{-1} = c_s^2(\alpha, p, \mathcal{S}). \quad (18.27)$$

Equations (18.26)–(18.27) replace (18.23) and (18.25); since the speed of sound is large compared to the meso-scale wave speeds and also is rather insensitive to its arguments (especially salinity), it plays a rather minor role in the large-scale dynamics.

In the appendix, we write the nondimensional forms of these equations based on a time scale T , a horizontal velocity scale U , a vertical velocity scale W , and a depth scale H . For the horizontal coordinates we introduce two scales of motion: the global, Θ and $\Phi \sim 1$ (the β -effect is global); and the local, $\Delta\Theta$ and $\Delta\Phi \sim L/a$, where L is a typical horizontal scale (cf. Phillips's 1973 WKB approach to Rossby waves). Thus we represent all dependent variables Q in the form $Q(\theta, \phi, z, t, \Theta, \Phi)$ with $d\phi = (a/L)d\Phi$ and $d\theta = (a/L)d\Theta$. We also explicitly introduce a basic hydrostatically balanced stratification of the ocean $\bar{T}(z)$, $\bar{\mathcal{S}}(z)$, $\bar{\alpha}(z)$, $\bar{p}(z)$ satisfying $\bar{\alpha}(z)\bar{p}(z) = -g$.

[In practice, given $\bar{T}(\bar{p})$, $\bar{\mathcal{S}}(\bar{p})$ we find $\bar{\alpha}(\bar{p})$ and integrate to get $z(\bar{p})$.] We then subtract out this hydrostatic state and define the (nondimensional) geostrophic streamfunction ψ by

$$p = \bar{p} + 2\Omega \sin \Theta UL \psi / \bar{\alpha}. \quad (18.28)$$

We also define a "local" potential specific volume α_p of a fluid particle with specific volume α at pressure p and depth z as the specific volume it would acquire if the particle moved adiabatically to the horizontally averaged pressure $\bar{p}(z)$. Equation (18.26) gives

$$\alpha_p = \alpha - \frac{\bar{\alpha}^2}{c_s^2} (\bar{p} - p) \quad (18.29)$$

(as long as α and p are not too different from their averaged values). The buoyant force per unit mass after this change becomes

$$\begin{aligned} b_p \text{ (dimensional)} &= g \frac{\alpha_p - \bar{\alpha}}{\bar{\alpha}} \\ &= g \frac{\alpha - \bar{\alpha}}{\bar{\alpha}} + g \frac{\bar{\alpha}}{c_s^2} (p - \bar{p}). \end{aligned}$$

This leads to a redefinition of the specific volume in terms of the nondimensional potential buoyancy:

$$\alpha = \bar{\alpha} \left[1 + \frac{2\Omega \sin \Theta UL}{gH} \left(b_p - \frac{gH}{c_s^2} \psi \right) \right].$$

With the above scalings, we have eight nondimensional parameters (many of which vary spatially):

$$\varepsilon = \frac{1}{2\Omega \sin \Theta T} \quad (\text{a time Rossby number}),$$

$$\epsilon = \frac{U}{2\Omega \sin \Theta L} \quad (\text{a velocity Rossby number}),$$

$$\hat{\beta} = (L/a) \cot \Theta,$$

$$\lambda = H/L,$$

$$\Delta = (2\Omega \sin \Theta L)^2 / (gH),$$

$$\Delta_s = gH / \bar{c}_s^2,$$

$$\omega = LW / (HU),$$

$$\hat{S} = H^2 \bar{N}^2(z) / (2\Omega \sin \Theta L)^2,$$

where \bar{N}^2 is the square of the buoyancy frequency:

$$\bar{N}^2 = [g\bar{\alpha}_z / \bar{\alpha}] - [g^2 / \bar{c}_s^2].$$

Two of these parameters, ϵ and $\hat{\beta}$, are identical to those used previously with the definitions $f_0 = 2\Omega \sin \Theta$ and $\beta = 2\Omega \cos \Theta / a$. We have also explicitly separated the time scale from the Rossby wave period, whereas in the previous section ε was set equal to $\hat{\beta}\hat{S}$ with $\hat{S} = gH / f_0^2$. The quantity analogous to \hat{S} for a continuously stratified ocean is

$$\hat{S} = H^2 \bar{N}^2(z) / (2\Omega \sin \Theta L)^2.$$

This nondimensional variable is of order unity for motions due to baroclinic instability (Eady, 1949). It is useful to think of it as the squared ratio of two length scales, L_R^2/L^2 or H^2/H_R^2 , where $L_R \sim \bar{N}H/f_0$ is the analog for a stratified ocean of the single-layer horizontal deformation radius \sqrt{gH}/f_0 introduced by Rossby (1938), and by analogy $H_R \sim f_0 L/\bar{N}$ may be called a vertical deformation radius. If the vertical scale is set, the natural horizontal scale will be L_R ; if the horizontal scale is set, the natural vertical scale will be H_R .

We now simplify the equations of motion by making assumptions about the magnitudes of the various parameters. The first seven of our nondimensional parameters are small (for the atmosphere, Δ_s may be of order 1). However, the stability parameter \hat{S} is quite variable. Taking $H \sim 1000$ m as a measure of the depth of the main thermocline, we find that \hat{S} is large in the seasonal thermocline and near unity in the main thermocline. Although this variability is occasionally worrisome in making scale arguments, we shall follow the conventional choice of regarding $\hat{S} \sim O(1)$.

We begin by restricting the length scale L so that $\lambda \ll 1$ and $\Delta \ll 1$, implying that L is large compared to the ocean depth but small compared to the external deformation radius $\sqrt{gH}/f_0 \sim 3000$ km. In practice, we expect the upper limit for L to be determined by the condition that $\hat{S} \gg O(\hat{\beta})$, so that L must be less than the intermediate scale L_1 defined in section 18.4.2. Using $\lambda \ll 1$ and $\Delta \ll 1$ and dropping small terms, we obtain the Boussinesq hydrostatic forms of the primitive equations (see the appendix).

Next we specify the time and velocity scale. For the standard quasi-geostrophic motions, the time scale is set by instabilities of the flow so that $T = L/U$ ($\varepsilon \sim \varepsilon$) and the vertical velocity is determined by balance between local and advective changes in the vertical component of relative vorticity and stretching of the vortex tubes of the earth's rotation ($\omega = \varepsilon$). Finally, the advective changes of the relative and planetary vorticity are assumed to be comparable, so that $\hat{\beta} \sim \varepsilon$ also. Expanding in ε , we find, as expected, that the lowest-order flows are geostrophic and hydrostatic:

$$u = -\frac{\partial \psi}{\partial y}, \quad v = \frac{\partial \psi}{\partial x}, \quad b_p = f_0 \frac{\partial \psi}{\partial z}, \quad (18.30)$$

where we have redefined the rapidly varying coordinates to look Cartesian by setting $dx = L \cos \Theta d\phi$ and $dy = L d\theta$ and have returned to dimensional variables. The full pressure is related to the streamfunction by

$$p = \bar{p}(z) + f_0 \psi / \bar{\alpha}(z). \quad (18.31)$$

The vorticity equation, which is derived by cross differentiating the order-Rossby number momentum equations (with special care taken with the Θ and Φ

dependence), and use of the order-Rossby number continuity equation, becomes

$$\left(\frac{\partial}{\partial t} + \mathbf{v} \cdot \nabla \right) (\nabla^2 \psi + \beta y) = f_0 w_z, \quad (18.32)$$

and the buoyancy equation becomes

$$\left(\frac{\partial}{\partial t} + \mathbf{v} \cdot \nabla \right) \psi_z + f_0 S w = 0. \quad (18.33)$$

Here $S = \bar{N}^2(z)/f_0^2$, $\mathbf{v} = (-\psi_y, \psi_x)$, and $\nabla = (\partial/\partial x, \partial/\partial y)$. These two may be combined to give the quasi-geostrophic equation

$$\left(\frac{\partial}{\partial t} + \mathbf{v} \cdot \nabla \right) \left(\nabla^2 \psi + \frac{\partial}{\partial z} \frac{1}{S} \frac{\partial}{\partial z} \psi + \beta y \right) = 0, \quad (18.34)$$

which asserts that the quantity

$$q = \nabla^2 \psi + \frac{\partial}{\partial z} \frac{1}{S} \frac{\partial}{\partial z} \psi + \beta y$$

is conserved at the projection of a particle in a horizontal plane, not, like potential vorticity, at the particle. For this reason it is called *pseudopotential vorticity* to distinguish it from potential vorticity. Because the distinction vanishes for a fluid consisting of several homogeneous incompressible or barotropic layers, there has been some confusion of terminology in the literature.

The temperature and salinity fields can be derived from the streamfunction ψ and the basic stratification $\bar{T}(z)$, $\bar{\mathcal{P}}(z)$, using the salinity and temperature equations together with the expression (18.33) for the vertical velocity:

$$\left(\frac{\partial}{\partial t} + \mathbf{v} \cdot \nabla \right) (\mathcal{S} - \bar{\mathcal{P}}) + w \bar{\mathcal{P}}_z = 0,$$

$$\left(\frac{\partial}{\partial t} + \mathbf{v} \cdot \nabla \right) (T - \bar{T}) + w \left(\bar{T}_z - \frac{g \bar{T} \bar{\alpha}_T}{\bar{\alpha} c_p} \right) = 0.$$

To complete the system of equations we need the boundary conditions. At the bottom boundary vertical velocities are forced by flow over topography:

$$w = \mathbf{v} \cdot \nabla b \quad \text{at } z = -H, \quad (18.35a)$$

where $H(\Theta, \Phi)$ is the (local) mean depth, the true bottom being at $z = -H + b$. For consistency, $|b|/H$ is required to be order ε . At the upper free surface $z = \eta$, the assumption that L is small compared to the external radius of deformation implies that the boundary conditions

$$\left. \begin{array}{l} D\eta/Dt = w \\ p = 0 \end{array} \right\} \quad \text{at } z = \eta$$

can be approximated simply by

$$w = 0 \quad \text{at } z = 0, \quad (18.35b)$$

with the surface displacement computed from

$$\eta = \frac{f_0}{g} \psi(x, y, 0).$$

Finally, on the side-wall boundaries it is necessary to set both the order 1 and order ε normal velocities to zero, giving

$$\begin{aligned} \nabla \psi \cdot \hat{s} &= 0, \\ \oint \nabla \psi_t \cdot \hat{n} &= 0, \end{aligned} \quad (18.36)$$

where \hat{s} is the unit tangent vector and \hat{n} the unit normal vector to the boundary.

All of these conditions will be modified in the presence of friction: the top and bottom layers because of Ekman pumping into or out of the frictional layer (see section 18.6) and the side conditions by the necessity for upwelling layers which can feed offshore Ekman transports and can accept mass flux from the interior of the ocean.

18.5 Linear Quasi-Geostrophic Dynamics of a Stratified Ocean

The quasi-geostrophic equations (18.33)–(18.36) have been applied to large-scale, long-period, free- and forced-wave motions in the atmosphere, to the study of barotropic and baroclinic instability, to wave-mean flow and wave-wave interaction, and to geostrophic turbulence. We have mentioned already the review articles by N. Phillips (1963) and Kuo (1973) and the book by Pedlosky (1979a) in which their applications are treated. In addition, Dickinson (1978) has reviewed their application to long-period oscillations of oceans and atmospheres and Holton (1975) their application to upper-atmosphere dynamics.

In application to the mesoscale eddy range of oceanic motions ($10 \text{ km} < L < 210 \text{ km}$), equations (18.32)–(18.36) exhibit a rich variety of behavior depending on the sizes of the various parameters and the initial and boundary conditions. We cannot discuss all of them here; rather we shall confine ourselves to a few topics which are also familiar in a meteorological context. We shall, whenever possible, use a typical oceanic $N^2(z)$ profile (Millard and Bryden, 1973; also see figure 18.7) rather than the constant- or delta-function profiles that are most commonly considered. This allows us to describe the vertical dependence of theoretical predictions in a way which is more directly comparable with oceanic data.

We begin with phenomena that are essentially linear—involving no transfers of energy between scales—deferring discussion of nonlinear motions to the next section.

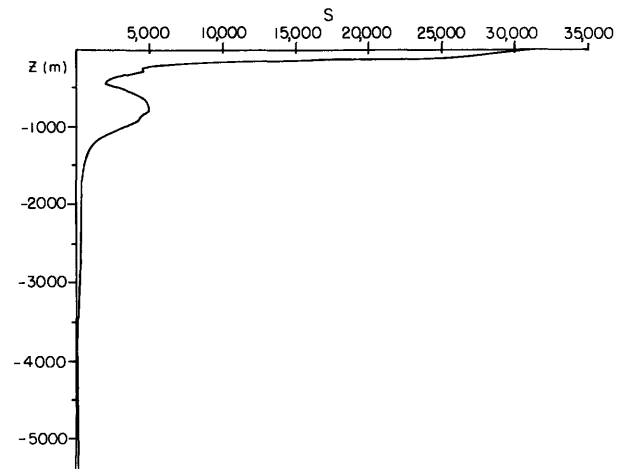


Figure 18.7 Typical oceanic structure for $S(z) = N^2/f_0$. The data are from Millard and Bryden (1973) and represent an average over ten stations centered on 28°N and 70°W .

18.5.1 Rossby Waves and Topographical Rossby Waves

Rhines (1970) has discussed the nature of free quasi-geostrophic waves in a uniformly stratified fluid with bottom topography in some detail. We shall describe the behavior of these waves with the aid of a formalism that permits us to extend Rhines's results to real $N^2(z)$ profiles.

When the bottom slope is uniform (b_x and b_y constant), the equations are separable, so that we can write the streamfunction in the form

$$\psi = AF(z) \sin[k(x - ct) + ly], \quad (18.37)$$

where

$$c = -\beta / (k^2 + l^2 + \lambda^2) \quad (18.38)$$

and λ , the separation constant, governs the z dependence:

$$\frac{\partial}{\partial z} \frac{1}{S} \frac{\partial}{\partial z} F = -\lambda^2 F. \quad (18.39)$$

To close the system, we make use of the boundary conditions

$$\frac{\partial}{\partial t} \psi_z = 0, \quad z = 0,$$

$$\frac{\partial}{\partial t} \psi_z = -f_0 S(-H) / (\psi, b), \quad z = -H,$$

which become

$$F_z = 0, \quad z = 0, \quad (18.40a)$$

$$\begin{aligned} F_z &= \frac{-f_0 S(-H)}{\beta} \left(b_y - \frac{1}{k} b_x \right) \\ &\quad \times (k^2 + l^2 + \lambda^2) F, \quad z = -H. \end{aligned} \quad (18.40b)$$

To solve (8.39) and (18.40) we proceed as follows: given $S(z)$ we integrate (18.39) with the boundary condition (18.40a) and the normalization condition

$$(1/H) \int_{-H}^0 dz F^2(z; \lambda^2) = 1$$

(using a simple staggered-grid difference scheme with 50-m vertical resolution). We then define the nondimensional function

$$R(\lambda^2) \equiv \frac{-HF_z|_{-H; \lambda^2}}{S(-H)F(-H; \lambda^2)} \quad (18.41)$$

in terms of which the bottom boundary condition (18.40b) becomes

$$R(\lambda^2) = \frac{f_0 H}{\beta} \left(b_y - \frac{1}{k} b_x \right) (k^2 + l^2 + \lambda^2). \quad (18.42)$$

This can be used to determine λ^2 and the vertical structure $F(z)$, given the wave scale $(k^2 + l^2)^{-1/2}$ and the propagation angle $\tan \theta = l/k$.

Thus, we can summarize all of the information in one graph. Figure 18.8 shows $R(\lambda^2)$, from which λ^2 can be determined given the wave numbers and the topographic slopes by a graphical solution of (18.42). From the resulting set of λ^2 values, the values of the phase speeds of the various waves can then be determined from (18.38). The vertical structures of the waves and

the dependence of their phase speeds on the slopes and wave numbers are qualitatively similar to those in Rhines's (1970) constant- N model. We shall describe these results and give useful approximate formulas for c .

When there is no slope effect, the λ_n values are simply the inverses of the deformation radii associated with the various modes $F_n(z)$ which are eigensolutions of (18.39) under the condition $F_z = 0$ for $z = 0, -H$, normalized so that $(1/H) \int_{-H}^0 dz F_n^2(z) = 1$. The barotropic ($n = 0$) and first baroclinic modes ($n = 1, L_R = 46$ km) correspond to the structures observed in oceanic data (cf. Richman, 1976). The vertical dependence of these structures are shown also in figure 18.8. The dispersion relation (18.38) and the propagation characteristics of the various modes are described in many places (see chapter 10).

For the weak topographic slope effect, the phase speeds are altered to

$$c = - \left[\beta + \frac{f_0 F_n^2(-H)}{H} \left(b_y - \frac{1}{k} b_x \right) \right] / (k^2 + l^2 + \lambda_n^2),$$

derived by solving (18.39) for $\lambda^2 - \lambda_n^2$ small. We find the familiar result that the bottom slope, by causing vortex stretching or shrinking, acts as an effective β . The bottom-slope effect in the baroclinic modes is weaker by a factor $F_n^2(-H)$ than the corresponding effect

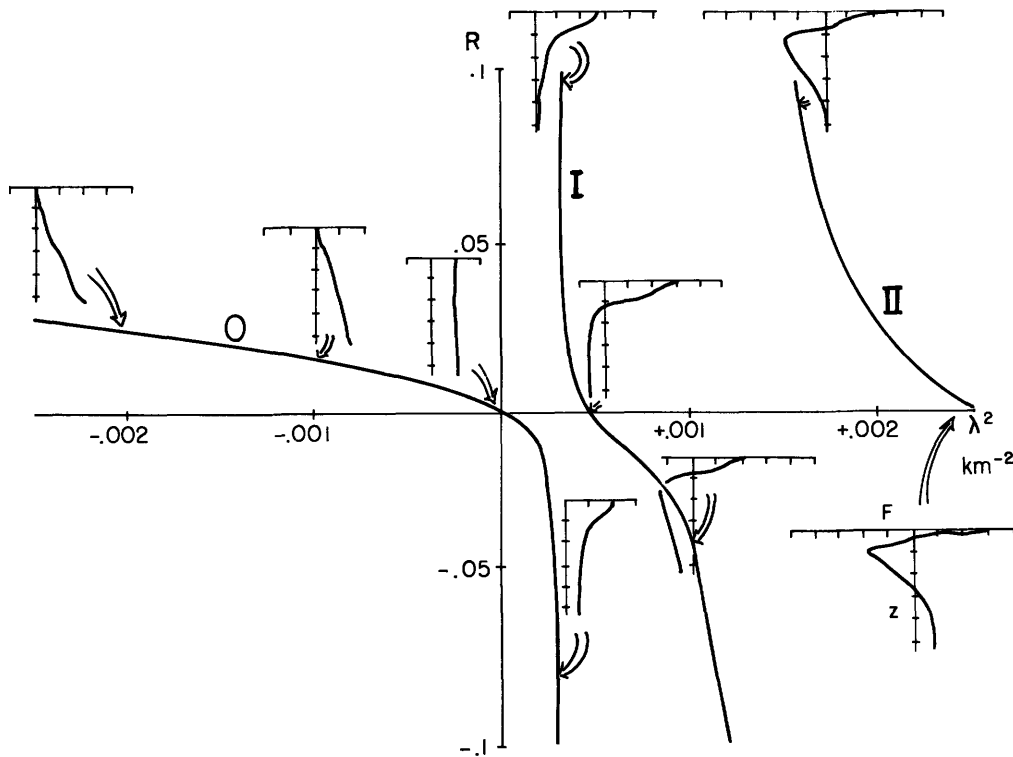


Figure 18.8 Normalized ratio of bottom shear to bottom amplitude as a function of the separation constant λ^2 . For given topographic slopes and wavenumber vector, the values of λ^2 are the intersections of this curve with the line $R =$

$(f_0 H / \beta) [b_y - (l/k) b_x] (\lambda^2 + k^2 + l^2)$. Also shown is the vertical structure $F(z)$ of the streamfunction (normalized to rms value unity) at various (λ^2, R) values.

on the barotropic mode. This factor is smaller than 1 for the stratification used (about 0.4 for the first baroclinic mode).

When the slope effect $f_0 H [b_y - (l/k)b_x]/\beta$ is negative, there is also a bottom-trapped eastward-moving wave. The vertical trapping scale is $H_s = - (f_0/\beta) [b_y - (l/k)b_x]$, and the speed

$$c = \beta N^2 (-H) H_s^2 / f_0^2$$

can be regarded as that of a long wave in a fluid with a deformation radius based on the vertical scale H_s and the local value of N .

For large slopes the modes all have large vertical shear. Most of them are surface trapped, having essentially zero bottom amplitude and a westward component of phase speed. For a slope effect opposing the β -effect, there is also a rapidly eastward-moving wave whose vertical trapping scale is $H_R = f_0/N(-H)\sqrt{k^2 + l^2}$ and whose propagation speed is

$$c = -f_0 (b_y - \frac{1}{k} b_x) / H_R (k^2 + l^2)$$

in the limit of $L \ll L_R$.

The constant N or two-layer models make significant qualitative errors in describing one or another of these types of behavior. The flat-bottom baroclinic modes in a constant- N model have bottom velocities comparable to the surface velocities; when a weak slope is added, this produces a large change in the vortex stretching and in the phase speed. Thus, the effect of the slope on the baroclinic modes is twice as great as on the barotropic mode, not, as in the realistic ocean, half as great. For large slopes the trapping scale for constant N is much smaller than the correct scale because $N(-H)$ is small compared to the average value of N which would be used in a constant N model. This results in an overestimate of the phase speed. The two-layer model generally misrepresents the eastward-traveling mode: for weak slopes, it is altogether absent, while for strong slopes the two-layer model predicts $c \sim (k^2 + l^2)^{-1}$ rather than the correct $(k^2 + l^2)^{-1/2}$ dependence.

Although we have derived the solutions (18.37)–(18.42) from the linearized equations, the individual waves are also finite amplitude solutions to the equations of motion (18.32)–(18.36) because both

$$\left(\nabla^2 + \frac{\partial}{\partial z} \frac{1}{S} \frac{\partial}{\partial z} \right) \psi \quad \text{and} \quad \psi_z$$

are proportional to ψ at each horizontal level. In fact, the nonlinearities in the equation of motion (18.34) will vanish for any set of waves having each of their wave vectors parallel or having the same total scale $(k^2 + l^2 + \lambda^2)^{-1/2}$. In the latter case, all the waves have the same phase speed so that the composite streamfunction pattern propagates uniformly. The nonlinearity in the bottom boundary condition likewise van-

ishes if all waves have the same value of R , that is, if the wavenumber vectors are parallel or $b_x = 0$. Thus sets of waves with horizontal scales $(k^2 + l^2)^{-1/2}$ such that both $k^2 + l^2 + \lambda^2 = \text{constant}$ and $R(\lambda) = \text{constant}$ will be full nonlinear solutions for north-south bottom slopes. Instabilities may, of course, prevent such patterns from persisting.

18.5.2 Generation of Rossby Waves by Flow over Topography

Flow over topography has been of practical interest to meteorologists attempting to forecast conditions near large mountain ranges for many years. There is an extensive bibliography of such studies (Nicholls, 1973; Hide and White, 1980). Many of these concentrate on smaller-scale lee-wave properties, although there have also been attempts to model the large-scale standing atmospheric eddies as topographically forced Rossby waves (cf. Charney and Eliassen, 1949; Bolin, 1950).

In the ocean, there are also many standing features, some of which clearly can be identified with topography (cf. Hogg, 1972, 1973; Vastano and Warren, 1976). In this section we shall discuss a simple oceanic analogy to the common atmosphere model for standing waves produced by flow over topography.

Steady solutions to (18.33)–(18.35) may be written

$$\begin{aligned} \nabla^2 \psi + \frac{\partial}{\partial z} \frac{1}{S} \frac{\partial}{\partial z} \psi + \beta y &= P(\psi, z), \\ \psi_z &= T_s(\psi), \quad z = 0, \\ \psi_z + f_0 S(-H)b &= T_b(\psi), \quad z = -H, \end{aligned} \quad (18.43)$$

where P , T_s , and T_b are arbitrary functionals. If we allow ψ to represent a mean zonal flow plus a topographically induced deviation,

$$\psi = -\bar{u}(z)y + \phi(x, y, z),$$

we find

$$P(\psi, z) = - \left(\beta - \frac{\partial}{\partial z} \frac{1}{S} \frac{\partial \bar{u}}{\partial z} \right) \psi / \bar{u},$$

$$T_s = T_b = 0$$

are suitable functionals to match the terms linear in y in (18.43). We have restricted ourselves to flows such that $\bar{u} \neq 0$ everywhere and $\bar{u}_z = 0$ at $z = 0, -H$. The conditions that the upper and lower surfaces be isothermal are not fundamental and could be relaxed easily; we make them simply to restrict the discussion to a reasonable number of parameters. If, however, the $\bar{u} \neq 0$ condition is violated, the analysis becomes much more difficult since the critical-layer (where $\bar{u} = 0$) problem must also be solved.

Given these restrictions, however, the fluctuation field satisfies the simple equations

$$\nabla^2 \phi + \frac{\partial}{\partial z} \frac{1}{S} \frac{\partial}{\partial z} \phi + \frac{\beta - (\partial/\partial z)(1/S)(\partial \bar{u}/\partial z)}{\bar{u}} \phi = 0,$$

$$\phi_z = 0, \quad z = 0, \quad (18.44)$$

$$\phi_z = -f_0 S(-H)b(x,y), \quad z = -H,$$

where no small-amplitude assumption has been made beyond the assumption that the nondimensional topographic amplitude is of the order of the Rossby number. The linearity of these equations is due to the particularly simple form of the upstream flow—a streamfunction field which is linear in y . Any horizontal shear in the upstream flow would give rise to nonlinear terms in P , T_s , and T_b , and thereby to nonlinearities in the equations (18.44). For simple sinusoidal topography $b = b_0 \sin(kx + ly)$, the topographically forced wave looks like

$$\phi = f_0 b_0 H F(z) \sin(kx + ly),$$

where

$$\frac{\partial}{\partial z} \frac{1}{S} \frac{\partial}{\partial z} F = \left[k^2 + l^2 - \frac{\beta - (\partial/\partial z)(1/S)(\partial \bar{u}/\partial z)}{\bar{u}} \right] F,$$

$$F_z = 0, \quad z = 0, \quad (18.45)$$

$$F_z = -S(-H)/H, \quad z = -H.$$

When the zonal flow is barotropic ($\bar{u} = \text{constant}$) the system (18.45) becomes essentially identical to (18.39)–(18.40) except that the amplitude is determined by the bottom boundary condition. We summarize the shapes and amplitudes of the forced waves in figure 18.9. We have used again the simplest form $\lambda^2 = \beta/\bar{u} - (k^2 + l^2)$ for the dependent variable.

The most striking feature in the response is, of course, the resonant behavior when

$$\bar{u} = \beta/(k^2 + l^2 + \lambda_n^2)$$

for λ_n^2 one of the inverse-square deformation radii. Near such a resonance, the amplitude becomes very large:

$$F(z) \approx \frac{F_n(z)F_n(-H)}{[k^2 + l^2 - (\beta/\bar{u}) + \lambda_n^2]H^2}.$$

When the mean flow is eastward at a few centimeters per second, it may be near a resonance for one of the baroclinic modes and may therefore generate substantial currents even above the thermocline. Vertical standing-wave modes associated with vertical propagation and reflection at the upper boundary will be found for $\lambda^2 > 0$ or

$$0 < \bar{u} < \beta/(k^2 + l^2).$$

For $\lambda^2 < 0$ the motions are trapped and decay away from the bottom. The trapping scale becomes very small when \bar{u} is nearly zero but westward or when the topographic wavelength is short. In the latter case, the

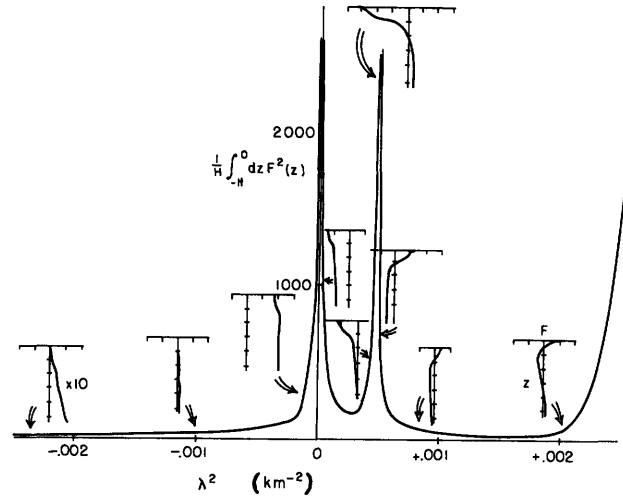


Figure 18.9 Energy and vertical structure of a topographically forced wave as a function of $\lambda^2 = (\beta/\bar{u}) - \mathbf{k} \cdot \mathbf{k}$, where \mathbf{k} is the topographic wavenumber.

vertical scale of the fluctuations is $H_R \sim f_0 L/N(-H)$, where $L = (k^2 + l^2)^{-1/2}$. When \bar{u} is weak and westward ($0 < |\bar{u}| < \beta N^2(-H)H^2/f_0^2 \sim 4$ cm s), the vertical scale will again be small compared to the fluid depth.

Although this type of problem is suggested by the atmosphere analogue, a warning about its applicability may be in order. Periodic problems are natural for the atmosphere. In the ocean, however, it is less plausible that a fluid particle periodically will revisit a topographic feature in a time less than the damping time for the excited wave. (The Antarctic Circumpolar Current could perhaps be an exception.) We can illustrate the differences between periodic and local topography by considering uniform eastward flow over a finite series of hills and valleys:

$$b = \begin{cases} b_0 \sin kx, & 0 \leq x \leq n\pi/k \\ 0, & x < 0 \text{ or } x > n\pi/k. \end{cases}$$

We consider the barotropic component of flow which satisfies the depth averaged form of (18.44):

$$\nabla^2 \hat{\phi} + \frac{\beta}{\bar{u}} \hat{\phi} = -\frac{f_0}{H} b(x,y).$$

Its solution is

$$\hat{\phi} = 0 \quad \text{for } x < 0,$$

$$\hat{\phi} = \frac{f_0 b_0}{H(k^2 - \beta/\bar{u})} \times \left(\sin kx - k \sqrt{\frac{\bar{u}}{\beta}} \sin \sqrt{\frac{\beta}{\bar{u}}} x \right)$$

$$\text{for } 0 < x < \frac{n\pi}{k},$$

$$\phi = \frac{f_0 b_0}{H(k^2 - \beta/\bar{u})} \times k \sqrt{\frac{\bar{u}}{\beta}} \left[\cos \sqrt{\frac{\beta}{\bar{u}}} x - (-1)^n \cos \sqrt{\frac{\beta}{\bar{u}}} \left(x - \frac{n\pi}{k} \right) \right]$$

for $x > \frac{n\pi}{k}$.

Figure 18.10 shows the average energy in the far field (normalized by $\frac{1}{2}(f_0 b_0/Hk)^2$) as a function of $\bar{u}k^2/\beta$. We note that the resonance peak becomes significant only when the topography has a number of hills and valleys; this suggests that the idea of resonance, in the ocean, should be applied with caution.

When there is vertical shear in the mean flow, the situation becomes somewhat different, although equation (18.45) can still readily be integrated. However, one can gain a qualitative picture of the response for arbitrary shear and small perturbations by using the methods of Charney and Drazin (1961) as described in the next section.

18.5.3 Propagation and Trapping of Neutral Rossby Waves

In many circumstances, the ocean or atmosphere is directly forced by external conditions—heating, winds—which may have temporal and spatial variations. The forcing may generate wave disturbances in one region that propagate into a neighboring region (e.g., the propagation of tropospheric disturbances into the stratosphere). In these circumstances the motion is determined by the nature of the forcing and the

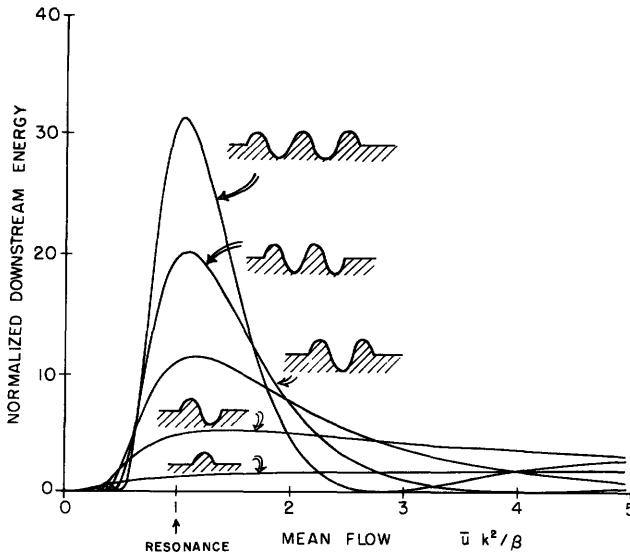


Figure 18.10 Downstream energy averaged over a wavelength of waves forced by flow over isolated bumps as a function of the normalized mean flow speed. The wavenumber of the topography in the region where it is varying is k . For an infinite topography, resonance would occur at $\bar{u}k^2/\beta = 1$. Results are shown for varying numbers of elevations and depressions in the topography.

refractive properties of the intervening medium. Charney (1949) first treated the vertical propagation of Rossby waves in a stratified atmosphere and Charney and Drazin (1961) first suggested the analogy between vertical propagation of Rossby waves and electromagnetic wave propagation in a medium with a variable index of refraction (possibly complex, corresponding to wave absorption). Holton (1975) has reviewed these concepts for meteorologists; oceanographers have tended to make less use of them [see, however, Wunsch (1977), who applied them to vertically propagating equatorial waves excited by monsoon winds].

The simplest derivation of an index of refraction is for waves in a zonal flow with vertical and horizontal shear. Consider waves of infinitesimal amplitude having east-west wavenumber k and frequency ω . The north-south and vertical dependencies of the amplitude $\psi = \Psi(y, z)e^{i(kx - \omega t)}$ are determined by the standard stability equation (cf. Charney and Stern, 1962):

$$\left(\bar{u} - \frac{\omega}{k} \right) \left(\frac{\partial^2}{\partial y^2} + \frac{\partial}{\partial z} \frac{1}{S} \frac{\partial}{\partial z} - k^2 \right) \Psi + \left(\beta - \bar{u}_{yy} - \frac{\partial}{\partial z} \frac{1}{S} \frac{\partial}{\partial z} \bar{u} \right) \Psi = 0.$$

If we follow the procedure that has been used for vertically propagating waves, we transform this into a Helmholtz equation with a variable coefficient of the undifferentiated term. This is quite straightforward if we are considering propagation only in the y direction with $\bar{u}_z = 0$ and $\Psi = \Phi(y)F_n(z)$, where F_n is one of the flat bottom eigenfunctions. Then the y structure is governed by

$$\frac{\partial^2}{\partial y^2} \Phi + \nu^2(y)\Phi = 0$$

where

$$\nu^2(y) = [(\beta - \bar{u}_{yy})/(\bar{u} - \omega/k)] - k^2 - \lambda_n^2. \quad (18.46)$$

A simple illustrative example is the radiation from a meandering Gulf Stream into the neighboring Sargasso Sea (cf. Flierl, Kamenkovich, and Robinson, 1975; Pedlosky, 1977). The forcing specifies Φ at some latitude. When we have no mean flow ($\bar{u} = 0$) and the motions are barotropic, the index of refraction becomes

$$\nu^2(y) = -k^2 - (\beta k/\omega)$$

The north-south scale of the response $|\nu|^{-1}$ is shown as a function of ω (>0) and k (≥ 0) in figure 18.11. Most observations indicate eastward-traveling motions, $\omega/k > 0$, implying that the mid-ocean response will be trapped close to the Gulf Stream.

We may obtain a similar representation of the index of refraction for the full two-dimensional (y and z) problem. This result, for reasons discussed below, is probably of more interest to meteorologists than to

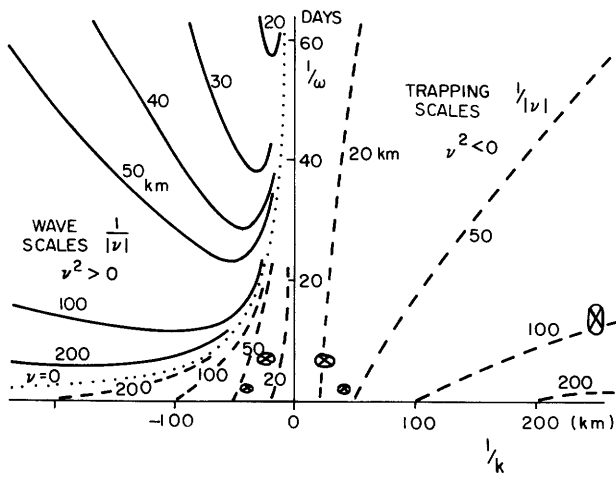


Figure 18.11 Solid lines show north-south length scales (wavelength/ 2π) and dashed lines shown trapping scales (e-folding distance) for barotropic waves generated by a meandering current with inverse frequency ω^{-1} and inverse wavenumber k^{-1} . Eastward going meanders ($k > 0$) produce trapped waves; westward going meanders ($k < 0$) may produce propagating disturbances. The symbols \otimes correspond to typical observational estimates of ω^{-1} and k^{-1} .

oceanographers; however, we include it to illustrate some of the effects of the z structure. If we substitute $\Psi(y, z) = S^{1/4}\Phi(y, \zeta)$, where $\zeta = \int_{z-H}^z S^{1/2}(z') dz'$ is a modified vertical coordinate, we find

$$\left(\frac{\partial^2}{\partial y^2} + \frac{\partial^2}{\partial \zeta^2}\right) \Phi + \nu^2(y, \zeta)\Phi = 0,$$

where the index of refraction $\nu^2(y, \zeta)$ is given by

$$\nu^2(y, \zeta) = S^{-1/4}[S^{-1}[S^{1/4}]_z]_z + \frac{\beta - \bar{u}_{yy} - (\bar{u}_z/S)_z}{\bar{u} - \omega/k} - k^2. \quad (18.47)$$

When $\nu^2 > 0$ there are sinusoidal solutions and energy propagates freely, whereas when $\nu^2 < 0$ there are only exponential solutions (along the ray) and the waves die out. There are also, of course, diffraction effects and tunneling effects if the regions of negative ν^2 (or, at least, significantly altered ν^2) are relatively small. This form is useful when N is a simple function (e.g., $N_0 e^{z/d}$) so that the first term in (18.47) is also simple $[-3/(4d^2S)]$. The stratification then contributes a relatively large and negative term which increases toward the bottom, inhibiting penetration into the deep water. For our $S(z)$ profile (figure 18.7), however, numerical differentiation proved to be excessively noisy. Moreover, in the oceans, most of the motions of interest have vertical scales that are significantly influenced by the boundaries and are larger than the scales of variation of ν^2 , so that a local (WKB) interpretation of ν^2 variations is not possible.

We can, however, associate modifications in ν^2 occurring on large scales with modifications in the structure of Ψ . Thus in the topographic problem, if the shear in the vertical is such that

$$\frac{\partial}{\partial z} \frac{1}{S} \frac{\partial \bar{u}}{\partial z} > 0 \quad \text{and} \quad \frac{\partial \bar{u}}{\partial z} > 0,$$

there will be a decrease in the value of ν^2 , implying that the wave will become either more barotropic ($\nu^2 > 0$) or more bottom trapped ($\nu^2 < 0$). In the example of Rossby wave radiation from a meandering Gulf Stream, (18.46) implies that the baroclinic modes ($\lambda_n^2 > 0$) become trapped even more closely than the barotropic modes.

As a final example, we note that the motions forced in the ocean by atmospheric disturbances tend to have large positive ω/k and large scales. In the absence of mean currents, the vertical structure equation, with $\Psi = e^{i\omega t} F(z)$, becomes

$$\frac{\partial}{\partial z} \frac{1}{S} \frac{\partial}{\partial z} F = \left[\frac{\beta k}{\omega} - k^2 - l^2 \right] F = -\nu^2 F, \quad (18.48)$$

implying that the forced currents are nearly barotropic. However, the recent work of Frankignoul and Müller (1979) suggests a possible mechanism by which significant baroclinic currents may be produced. Because the ocean is weakly damped and has resonant modes ($\nu^2 = \lambda_n^2$), even very small forcing near these resonances can cause the energy to build up in these modes. This is another example of the strong influence of the boundaries on the oceanic system.

18.6 Friction in Quasi-Geostrophic Systems

18.6.1 Ekman Layers

Ekman (1902, 1905), acting on a suggestion of Nansen, was the first to explore the influence of the Coriolis force on the dynamics of frictional behavior in the upper wind-stirred layers of the oceans. He considered both steady and impulsively applied, but horizontally uniform, winds. In an effort to understand how surface frictional stresses τ influence the upper motion of the atmosphere and, in particular, how a cyclone "spins down," Charney and Eliassen (1949) were led to consider horizontally varying winds. They showed that Ekman dynamics generates a horizontal convergence of mass in the atmospheric boundary layer proportional to the vertical component of the vorticity of the geostrophic wind in this layer. Thus a cyclone produces a vertical flow out of the boundary layer which compresses the earth's vertical vortex tubes and generates *anticyclonic* vorticity. The time constant for frictional decay in a barotropic fluid was found to be $(f_0 E^{1/2})^{-1}$, where E is the Ekman number $\nu_e / f_0 H^2$, with ν_e the eddy coefficient of viscosity and H the depth of the fluid. Greenspan and Howard (1963) investigated the time-